Geomorphology 490 (2025) 110010

Contents lists available at ScienceDirect

Geomorphology

journal homepage: www.journals.elsevier.com/geomorphology

Applying deep learning for boat detection and numerical modeling to assess sand mining impacts on river morphology: A case study in the Vietnamese Mekong Delta

Thi Huong Vu [a,*], Lars Backhaus [a], Doan Van Binh [b], Sameh Ahmed Kantoush [c], Jürgen Stamm [a]

[a] Faculty of Civil Engineering, TUD | Dresden University of Technology, 01069, Dresden, Germany
[b] Faculty of Engineering, Vietnamese-German University, Ho Chi Minh City, Viet Nam
[c] Disaster Prevention Research Institute, Kyoto University, Uji-shi, Kyoto, Japan

ARTICLE INFO

Keywords:
Boat detection
Delft3D-FLOW
River morphology
Sand mining impact
Vietnamese Mekong Delta

ABSTRACT

Effective management of riverbed sand mining is challenged by the lack of comprehensive data on sand mining volumes and their morphological impacts. This study presents an integrated framework combining deep learning, satellite imagery, and numerical modeling to monitor and assess the impacts of sand mining on river morphology in the Vietnamese Mekong Delta. A deep learning model was trained using Sentinel-1 imagery in 2023 to classify three boat types: Barge with Crane (BC), Sand Transport Boat (STB), and others. The model was then applied to detect BCs from 2014 to 2023, and the sand extraction volumes and areas were estimated. Finally, a Delft3D-FLOW model was employed to simulate the impacts of sand mining in the study period. Our deep learning model identified 386 BCs operating on the Bassac River in 2014–2023, with a total of 92.68–137.59 Mm^3 of extracted sand, averaging 10.02–14.87 Mm^3 annually. The numerical modeling results revealed significant riverbed incision, with a maximum annual net volume loss of −29.48 Mm^3/yr and a mean erosion rate of up to −0.82 m/yr. In addition, excessive sand mining formed 23 scour holes with depths up to 11 m and incised the thalweg at rates of up to −1.18 m/yr. Sand mining maximally contributed 41.0–56.4 % of total riverbed incision during 2014–2023. These findings underscore the urgent need for improved sediment management strategies and regulatory frameworks. By providing a comprehensive assessment of sand mining impacts, this study supports the development of sustainable river management strategies in the region.

1. Introduction

Sand mining has experienced a significant surge globally, with demand tripling annually over the past two decades to approximately 50 billion tons (UNEP, 2023). This escalation is driven primarily by urbanization and infrastructure development, leading to extensive extraction activities across rivers, beaches, and floodplains. However, unregulated and excessive sand extraction can lead to severe environmental and geomorphological consequences, including bed incision, riverbank erosion, habitat destruction, and salinity intrusion in delta rivers (Kondolf, 1997; Hackney et al., 2020; Loc et al., 2021; Binh et al., 2022). Many major rivers worldwide have been facing severe consequences from sand mining, such as the Mekong River in Vietnam and the Yangtze River in China (WMF, 2018), the Amazon River in Brazil (Ferrer et al., 2021), and the Narmada River in India (Roy et al., 2023).

The Vietnamese Mekong Delta (VMD) is the largest and most crucial delta in Vietnam, ensuring national food security, and is home to nearly 19 million people (Day et al., 2016; Quan et al., 2018; Binh et al., 2020b; Jordan et al., 2020; Dang et al., 2021). However, its sustainability is increasingly threatened by anthropogenic activities. In addition to upstream dam impacts, unsustainable sand mining in the delta's rivers caused severe environmental consequences (Gruel et al., 2022; Lau et al., 2023). It locally accelerates riverbed incision and riverbank erosion (Kondolf, 1997; Anthony et al., 2015; Binh et al., 2022; Lau et al., 2023), while broadly disrupting sediment transport and degrading the delta system (Binh et al., 2022; Xin et al., 2024). Sand extraction volumes have surged from 7.75 to 53.25 Mm^3/yr between 2012 and 2022 (Bravard et al., 2013; Jordan et al., 2019; Gruel et al., 2022; Kumar et al., 2024), while the delta annually receives about 40.0–166.7 Mt/yr of suspended load and 3 Mt/yr of bed load (Stephens et al., 2017; Binh

* Corresponding author.
E-mail address: thi_huong.vu@tu-dresden.de (T.H. Vu).

https://doi.org/10.1016/j.geomorph.2025.110010
Received 9 May 2025; Received in revised form 6 September 2025; Accepted 7 September 2025
Available online 11 September 2025

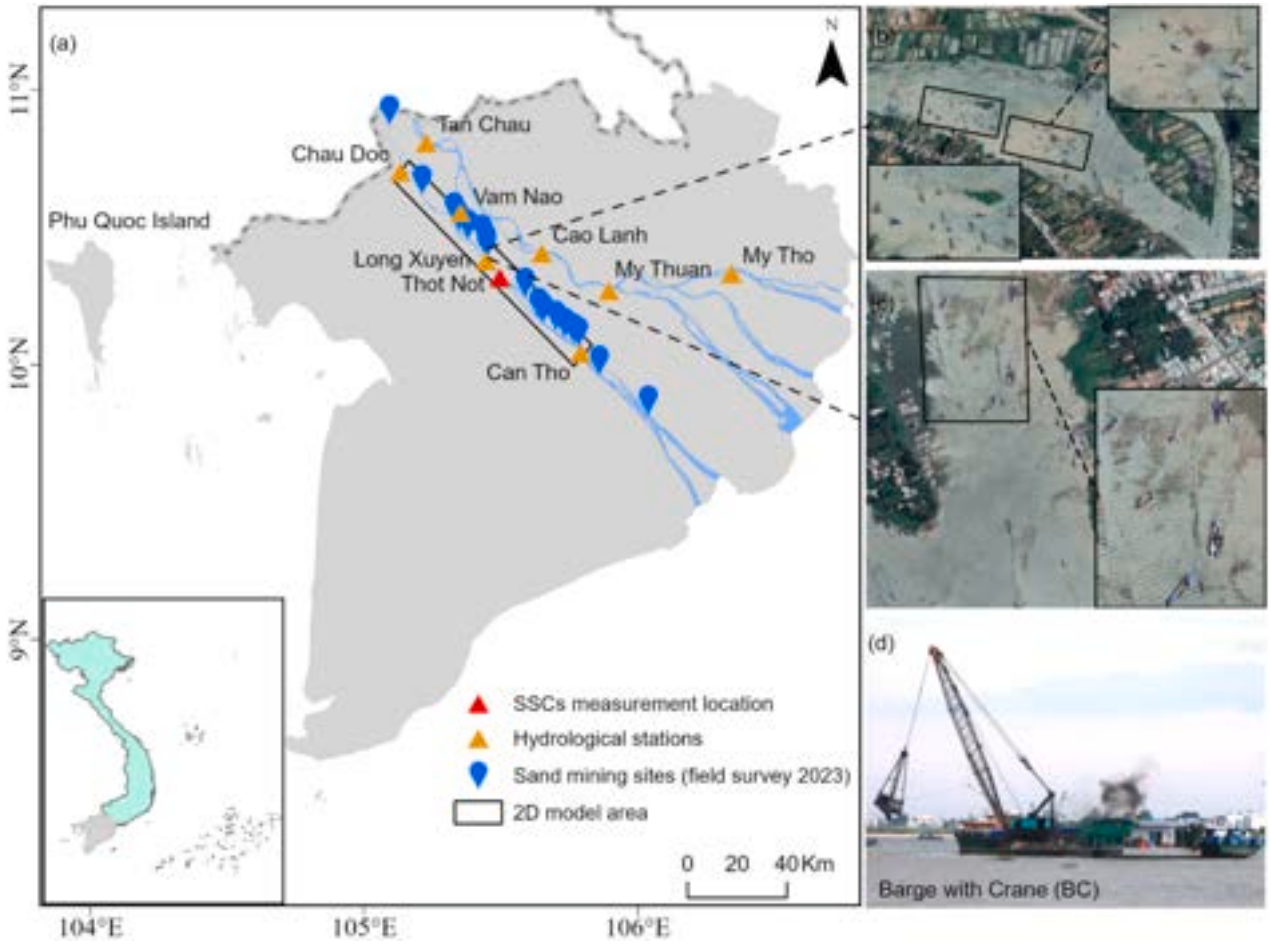

Fig. 1. (a) Map of the VMD. (b) and (c) Google Earth images showing some sand mining sites in 2023. (d) A BC's photo used for sand mining activity from the riverbed in the Bassac River, taken by Thi Huong Vu during a field survey on May 12, 2023.

et al., 2020b). Therefore, monitoring and managing sand mining activities are crucial for mitigating these adverse effects and ensuring sustainable resource use. However, effective tracking and assessment of sand mining remain challenging due to the lack of comprehensive monitoring frameworks.

Existing studies have provided valuable insights into both sand mining budgets and their effects on river morphology in the VMD. However, these studies tend to address these two aspects separately, lacking an integrated approach that tracks sand extraction from volume estimation through to its geomorphic consequences. Accurate estimation of sand mining volumes usually requires extensive bathymetric surveys (Brunier et al., 2014; Jordan et al., 2019), which are expensive and time-consuming, especially in large or complex river systems (Kumar et al., 2024). To avoid these challenges, some studies have relied on statistical reports of sand mining licenses (Eslami et al., 2019; Jordan et al., 2019). However, in the VMD, these figures are often significantly underestimated due to the prevalence of unregulated and illegal extraction activities (Lau et al., 2023; Kumar et al., 2024; Yuen et al., 2024). In response, more recent efforts have shifted toward remote sensing techniques. Estimating sand mining volumes through vessel detection in remote sensing imagery has emerged as a promising alternative, as it directly captures active extraction activities, allows wider spatial coverage, provides consistent temporal data, and is both scalable and feasible in data-scarce regions (Park, 2024). For example, Hackney et al. (2021) estimated sand extraction in Cambodia by manually counting Sand Transport Boats (STBs) in monthly PlanetScope imagery and using boat carrying capacity. While promising, this method is prone to uncertainty due to mapping rapidly moving boats with monthly satellite imagery. Gruel et al. (2022) improved this approach by manually counting the BCs on Google Earth images and creating a boat density map correlated to bathymetric changes. However, these manual approaches are labor-intensive and impractical for large-scale, long-term monitoring. To overcome such limitations, Kumar et al. (2024) further advanced this method by using deep learning to automatically detect BCs and generate density maps, which were then correlated with bathymetric changes to determine the sand mining volume. Although this method improved scalability, it assumed that all observed bed erosion was caused by sand mining, which may lead to overestimation in areas like the VMD, where upstream dam operations and other factors also contribute to sediment loss (Anthony et al., 2015; Darby et al., 2016; Binh et al., 2022; Lau et al., 2023). Furthermore, this approach depends on long-term bathymetric datasets, limiting its application in data-scarce environments. In numerical modeling, sand mining impacts on the river morphology are often simulated by directly altering the riverbed elevation of the sand mining area in proportion to the total sand mining volume, creating deep holes in the initial riverbed elevation at the beginning of the simulation (Kim et al., 2025; Nguyen et al., 2025). However, this approach overestimates the impact and does not reflect the gradual evolution of the riverbed under the impact of sand mining over time, as the extraction process occurs gradually rather than instantaneously (Nguyen et al., 2025).

To address these limitations, this study aims to develop a comprehensive framework for monitoring and assessing the impacts of sand mining on the river morphology. This framework represents a novel contribution by integrating the quantification of sand mining with the evaluation of its geomorphic impacts, thereby providing a

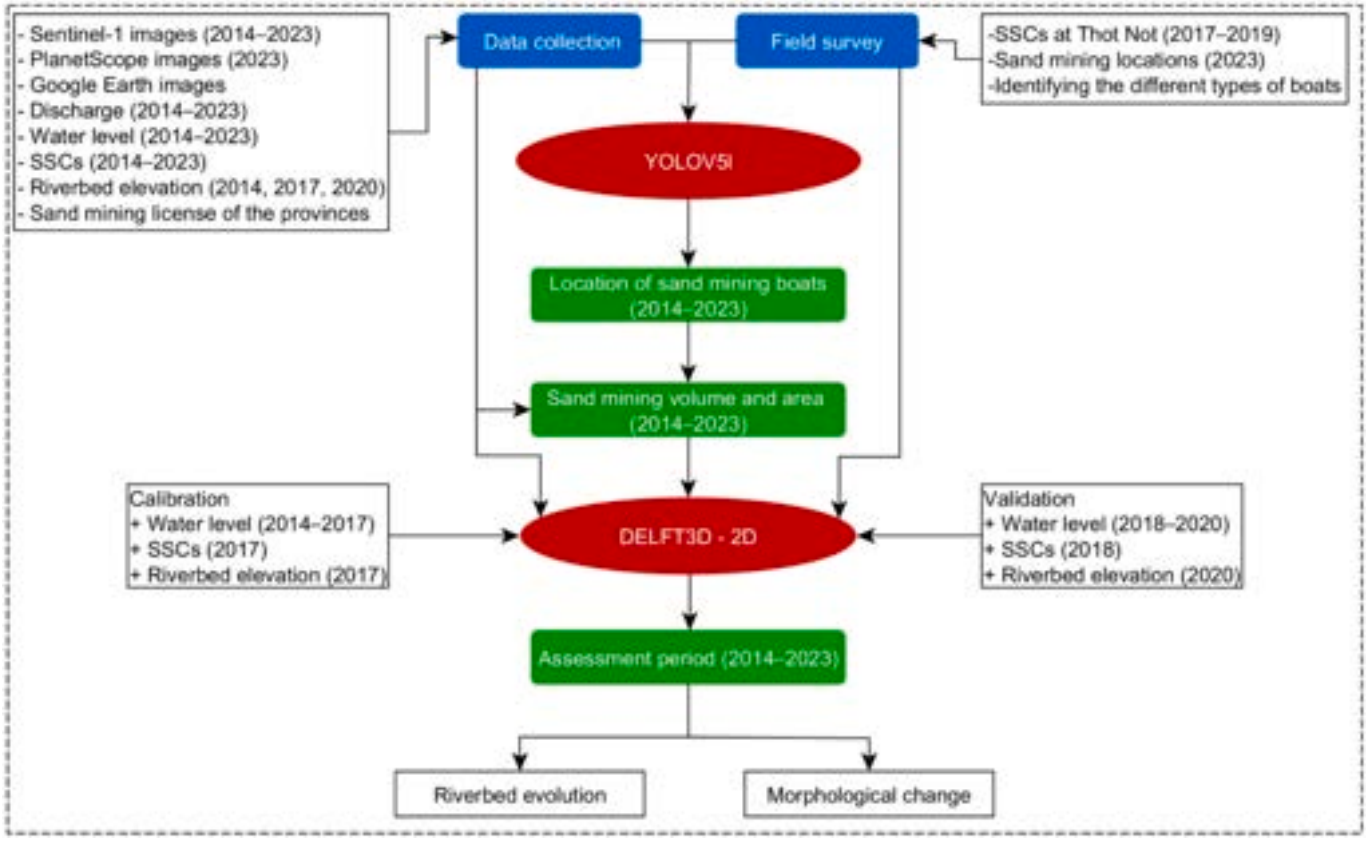

Fig. 2. Methodological framework of the research.

Table 1
Illustrations of the BC, STB, and Other boats from the four sources. Ground observation photos in the Bassac River were taken by Thi Huong Vu during a field survey on May 12, 2023.

Boat type	Ground observation	Google Earth image	PlanetScope	Sentinel-1
Barge with Crane (BC)				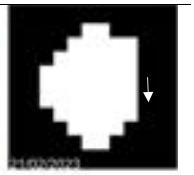
Sand Transport Boat (STB)				
Other (e.g., Cargo, fishing)				

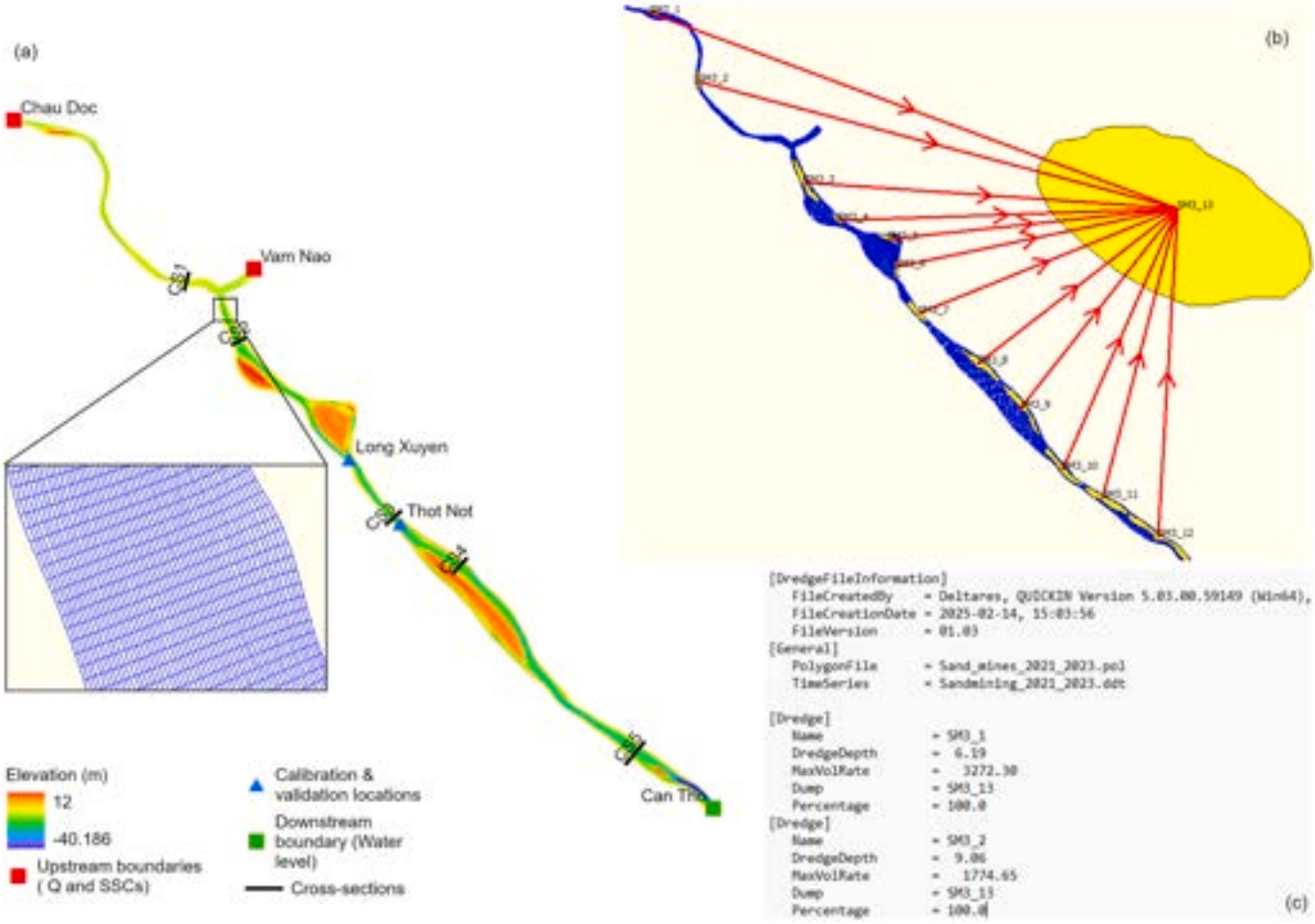

Fig. 3. (a) The simulated domain, mesh, geometry, boundaries, and calibration and validation locations. (b) and (c) Set up sand mining mines in the DELFT3D model.

comprehensive assessment that has been missing from prior research. The study focuses on three main objectives: 1) monitoring sand mining activity via the YOLOv5l deep learning model to detect sand mining boats, 2) estimating sand mining volumes at multiple scales (the Bassac River, provincial levels, and individual mines), and 3) simulating long-term morphological impacts of sand mining via Delft3D, incorporating dynamic changes in sand mining volumes over time. The YOLO-based detection method follows an approach previously applied by Kumar et al. (2024) but with different and more comprehensive training datasets compared to Kumar et al. (2024). The sand mining volumes were estimated by calculating extraction rates based on BC capacity and duration of mining activities, and then, a new empirical formula was proposed to estimate the volume of sand mining. This study's estimated sand mining volume was compared with that reported in past studies. Finally, to overcome the limitations of the previous research on modeling sand mining impacts, this study employed the dredging and dumping module in Delft3D, which was previously applied in global river systems, to assess long-term sand mining impacts in the VMD.

2. Study area

The Mekong River, one of the longest rivers in the world, flows through five countries before entering Vietnam and flowing into the East Vietnam Sea. The VMD, with a 39,000 km^2 area, has two main branches, namely the Mekong (length of 250 km) and Bassac Rivers (length of 220 km), which are linked by the Vam Nao River (Binh et al., 2021). The hydrological regime in the VMD has dry (January–June) and flood (July–December) seasons, with average discharges of approximately 1500 and 45,000 m^3/s, respectively.

Suspended sediment makes up the majority of the total sediment load of the VMD, with bedload accounting for only 1–3 % (Koehnken, 2014; Stephens et al., 2017). The VMD's average annual suspended sediment load (SSL) ranges from 40.0 to 166.7 Mt/yr, compared to an estimated 3.0 Mt/yr for the bed load. The flood season contributes approximately 99 % of the annual sediment load, with a peak in September accounting for 25–40 % of the total, whereas low-flow seasons contribute less than 1 % (Koehnken, 2014).

The application scope of the deep learning model covered the main rivers in the VMD, from the borders to the estuary. However, the sand mining volume was only estimated for the Bassac River, and the application of the 2D model to estimate the impact of sand mining activities was applied to the Bassac River from Chau Doc to Can Tho stations because of the available boundary conditions and the extensive sand mining activities in this reach (Fig. 1).

3. Materials and methods

3.1. Methodological framework

This study integrated collected data and field surveys to develop deep learning and numerical modeling for estimating sand mining boat locations, extraction volumes, and their impacts on riverbed elevation and morphological changes. Field surveys identified different boats and sand extraction sites, while satellite imagery supported the application

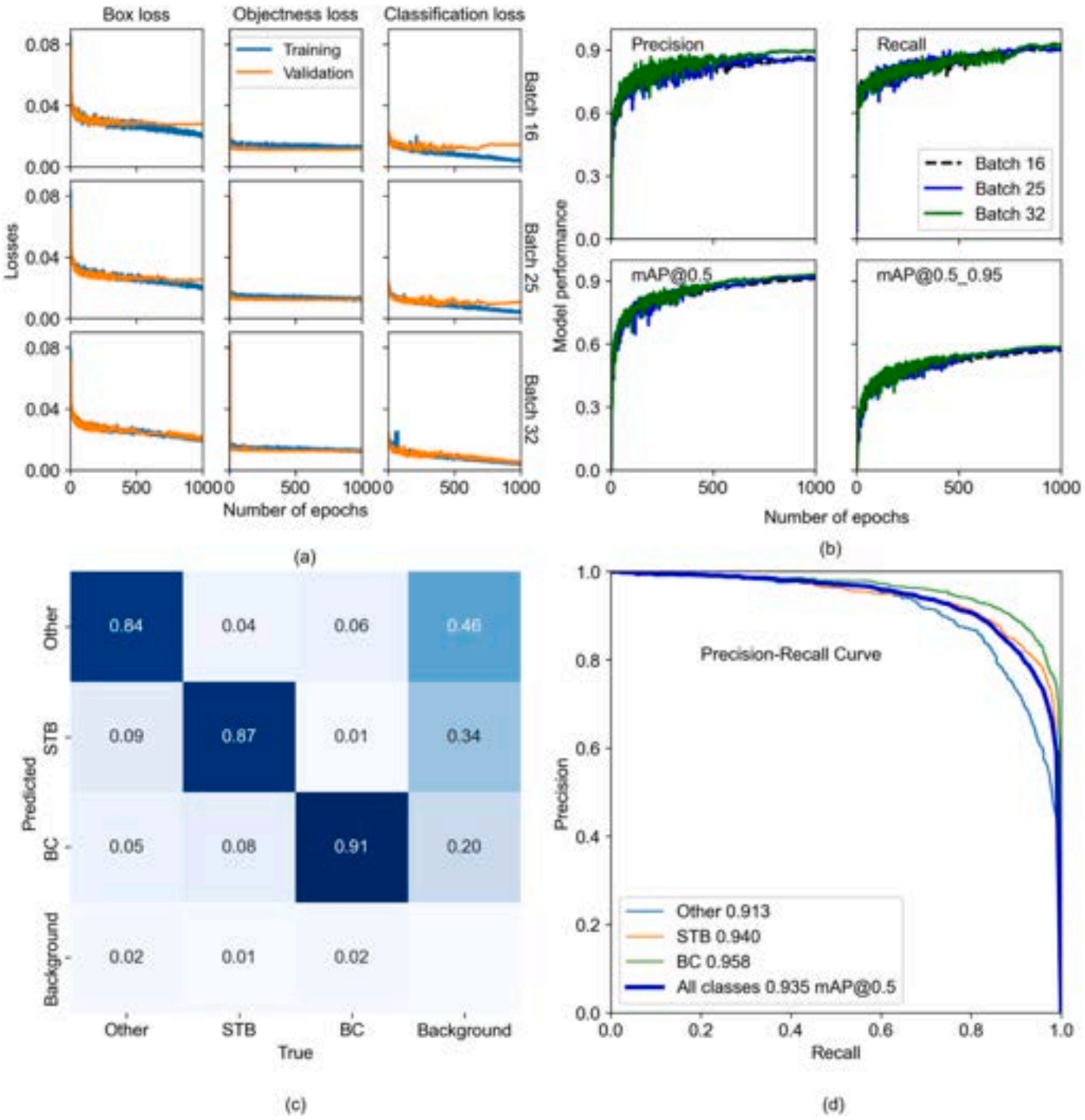

Fig. 4. Evaluation of deep learning model performance. (a) Loss curves during training and validation processes. (b) Model accuracy trends for various batch sizes (16, 25, and 32). (c) and (d) Confusion matrix and precision-recall curve for batch size 32 on the validation dataset, respectively.

Table 2
Deep learning performance training with the batch size 32 on the validation dataset.

Class	Images	Instances	P	R	mAP50	mAP50–95
all	270	2415	0.88	0.86	0.935	0.57
Other	270	1281	0.92	0.83	0.913	0.51
STB	270	910	0.88	0.85	0.940	0.56
BC	270	224	0.83	0.89	0.958	0.66

of a deep learning model to detect sand mining boats in the VMD. On the basis of the boat locations and the sand mining capacity and duration, the sand mining volumes and areas were calculated. Riverbed elevation from the field surveys, flow discharge, and suspended sediment concentration (SSC) data from the selected hydrological stations were used to establish the Delft3D-FLOW model. The Delft3D-FLOW model (2D), coupled with the dredging and dumping module, was utilized to simulate the impacts of sand mining for 2014–2023, assessing long-term riverbed incision and morphological changes in the Bassac River. The detailed study process is illustrated in Fig. 2.

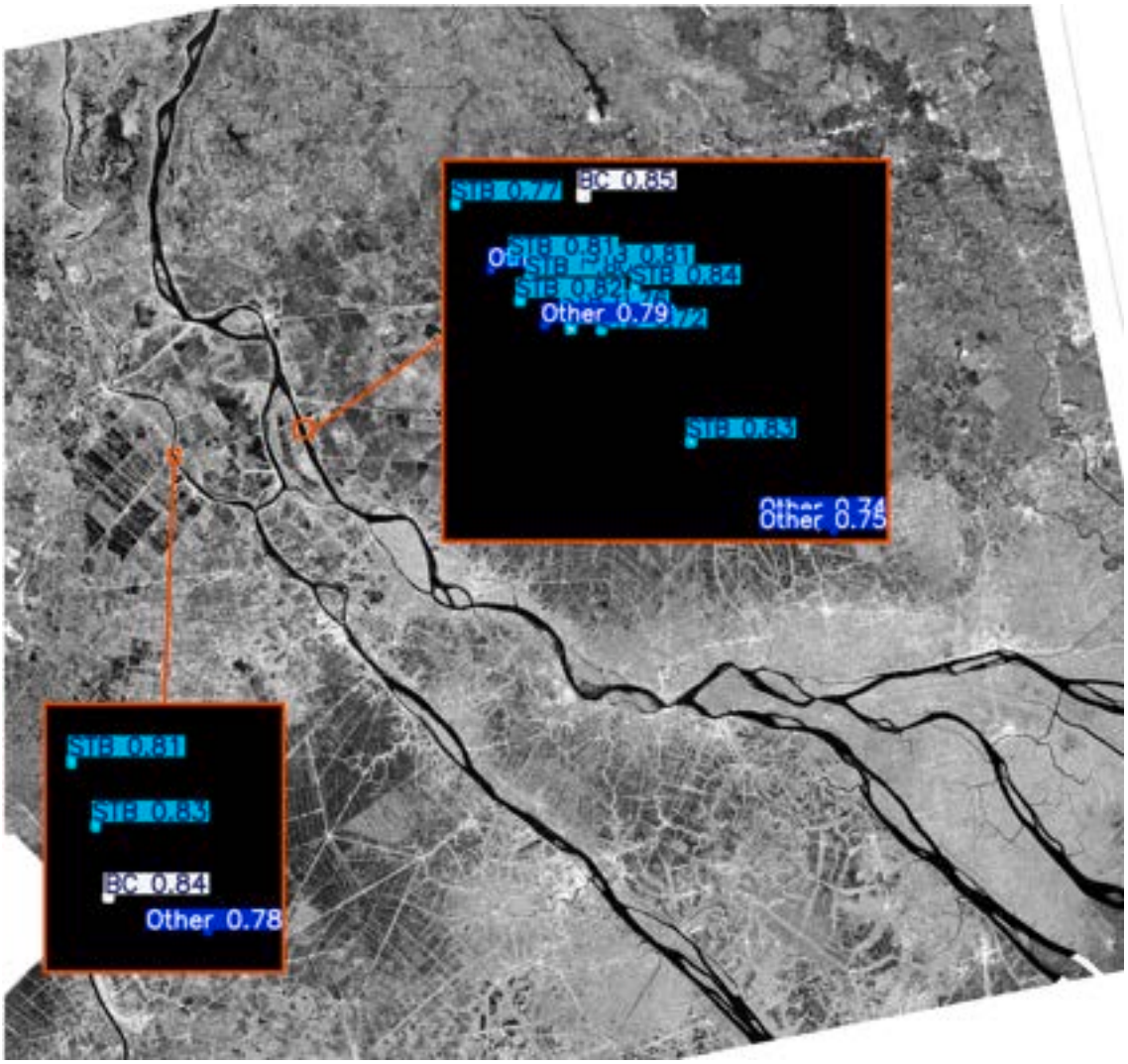

Fig. 5. Illustration of the predicted boat results with associated confidence scores using the YOLOv5l model. The background is the Sentinel-1 image.

3.2. Field surveys in the VMD

Field surveys were implemented in the Bassac and Vam Nao Rivers in 2014, 2017, 2018, 2019, 2020, and 2023. In 2014, the Southern Institute of Water Resources Research, Vietnam, used acoustic Doppler current profiler (ADCP) measurements to survey 375 cross-sections with 200–1000 m spacing. In August and September 2017, a JASTIP-funded survey measured riverbed elevations at 43 cross-sections via an ADCP (Binh et al., 2020a). The 2020 survey by the Southern Institute of Water Resource Planning collected 29 cross-sections at 3–5 km intervals via a Teledyne Odom Hydrotrac II (Ahmed et al., 2025).

In the simulation domain of the Bassac River from Chau Doc to Can Tho Stations, there are no SSC monitoring stations from authorities. Therefore, to enhance the calibration and validation of the morphodynamics model, the authors monitored SSC data via an INFINITY-Turbi ATU75W2-USB instrument from 10 February 2017 to 19 January 2019 at the Thot Not location (Fig. 1a).

Additionally, a field survey was conducted from May 1 to 15, 2023, to capture photographs of various boats, especially BCs (Fig. 1d), with their geographical locations. These photographs aided in identifying boats in satellite images to develop a deep-learning training dataset.

3.3. Sand mining boat detection via YOLO model

3.3.1. Data collection and preprocessing

Sentinel-1, developed by the European Space Agency (ESA) and launched in 2014, provides radar imagery for earth observations, functioning both day and night, under all weather conditions. Depending on the area observed, the system provides spatial resolutions of 10–40 m. The Sentinel-1 consists of three satellites: Sentinel-1A (S1A), launched on April 3, 2014; Sentinel-1B (S1B), launched on April 25, 2016, and decommissioned in 2022; and Sentinel-1C (S1C), launched in 2024. The revisit frequency with S1A and S1B combined was $\leq$5 days (ESA, 2014).

Sentinel-1 operates in four main imaging modes—strip map (SM), interferometric wide swath (IW), extra-wide swath (EW), and wave (WV)—with each mode offering data in three processing levels: Level 0, Level 1, and Level 2. For this study, Level-1 ground range detected (GRD) products were utilized, acquired in IW mode with dual polarization (VV + VH) at a C-band frequency of approximately 5.5 GHz (Kumar et al., 2024). The Sentinel-1 datasets were obtained from the Alaska Satellite Facility (ASF) portal (https://search.asf.alaska.edu/#/, accessed on 15 March 2024) by selecting the dates and target areas of images. Only images covering most of the VMD were selected, resulting in 635 images (October 6, 2014–December 31, 2023) with 10 m resolution. Data was preprocessed via the Sentinel Application Platform

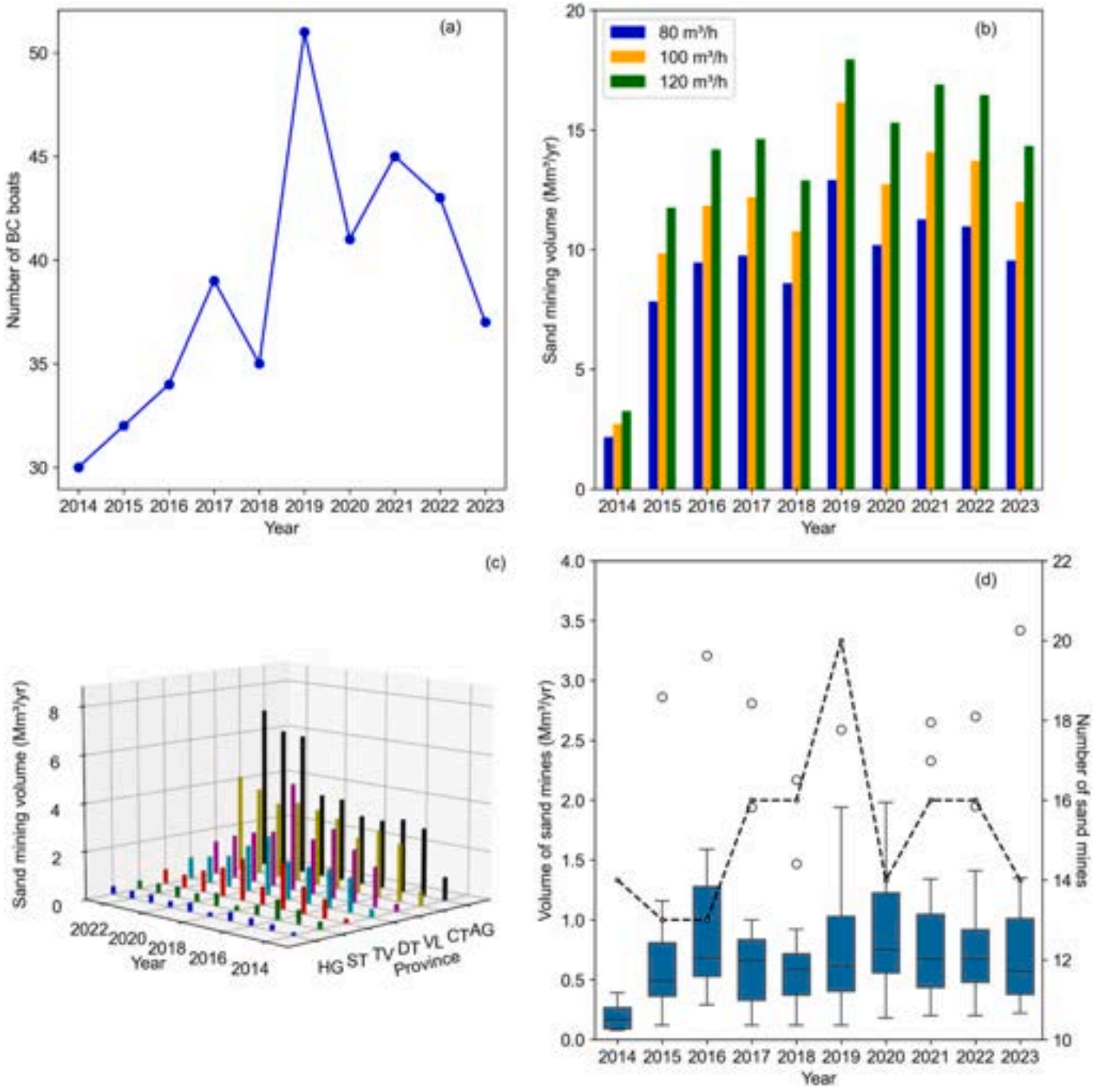

Fig. 6. Dynamics of sand mining boats and sand mining volume in the Bassac River in 2014–2023: (a) The annual number of BC boats. (b) The annual sand mining volume corresponding to boat capacities of 80, 100, and 120 m^3/h. (c) The annual sand mining volume across the provinces for the boat capacity of 100 m^3/h. (d) The number and the annual volume of sand mines for the boat capacity of 100 m^3/h.

(SNAP v8.0), a widely used toolbox developed by Brockmann Consult, SkyWatch, and C—S (Brockmann Consult, 2015).

Detecting different boat types for Sentinel-1 images is challenging because of their grayscale nature and low spatial resolution (Kumar et al., 2024). This study combined data from Sentinel-1, PlanetScope, Google Earth imagery, and field surveys to increase classification accuracy. The imagery of Sentinel-1, PlanetScope, and Google Earth from 2023 was selected to align with the timing of the field survey. Since PlanetScope images are affected by cloud cover and nighttime constraints, eight cloud-free PlanetScope images (on January 28, February 21, March 05, March 17, April 23, November 01, November 25, and December 18 in 2023) and corresponding Sentinel-1 images were selected for analysis in the VMD. Integrating with field surveys and Google Earth imagery, the boats in the PlanetScope and Sentinel-1 on the same date were classified into three categories: BC, STB, and Other, contributing to developing a deep-learning training dataset (Table 1). The reason for choosing only three different categories and the detailed boat classification method followed the approach of Kumar et al. (2024).

3.3.2. *Deep learning model development*

The YOLO (You Only Look Once) model is a widely used approach in object detection, with multiple versions developed over time. YOLOv5 enhances feature retention within its extraction network and optimizes algorithmic details, making it more robust and stable for detecting small

Table 3
Detailed information of sand mines in the VMD for Sc1.

Period	Sand mines	Area (ha)	Total volume (Mm^3)	Total volume per day (m^3)	Mining depth limit (m)
2014–2017	SM1_1	94.70	0.12	991.87	8.75
	SM1_2	37.39	2.82	2436.27	7.56
	SM1_3	63.93	1.76	1522.64	7.61
	SM1_4	334.03	4.99	4688.60	12.46
	SM1_5	610.20	9.74	8429.79	13.44
	SM1_6	424.98	4.95	4399.56	15.74
	SM1_7	76.16	1.56	1385.93	24.45
2018–2020	SM2_1	59.84	0.94	1816.28	9.32
	SM2_2	19.14	1.34	2087.73	7.49
	SM2_3	64.53	0.17	1357.72	7.73
	SM2_4	163.38	4.98	4551.75	12.93
	SM2_5	129.30	0.73	5926.83	8.06
	SM2_6	493.57	0.70	2909.09	5.05
	SM2_7	130.98	6.73	6149.47	13.26
	SM2_8	359.48	1.71	2671.61	17.21
	SM2_9	197.19	0.82	1687.97	17.92
	SM2_10	157.19	10.85	9905.78	19.35
	SM2_11	93.98	1.89	2585.39	13.08
2021–2023	SM3_1	71.20	1.39	3272.30	6.19
	SM3_2	47.54	1.78	1774.65	9.06
	SM3_3	88.66	3.01	2998.26	12.10
	SM3_4	91.88	0.95	1071.73	14.16
	SM3_5	150.46	8.78	8488.48	5.54
	SM3_6	82.33	5.63	5451.02	6.25
	SM3_7	200.03	0.53	1577.61	15.08
	SM3_8	232.07	1.04	1810.19	13.63
	SM3_9	344.08	2.35	2345.12	15.72
	SM3_10	364.21	1.65	1756.46	17.00
	SM3_11	354.82	3.13	3124.04	15.07
	SM3_12	163.23	6.56	6341.41	22.06

objects (Wang et al., 2024). This study utilized the YOLOv5l model because of its compact size and fast processing speed (Jocher et al., 2021; Ren et al., 2022). The model employs a CNN-based architecture with three key components: backbone (feature extraction), neck (feature aggregation via PANet), and head (object detection) (Jocher et al., 2021).

Following the approach of Kumar et al. (2024), the training and validation data for the deep learning model were prepared in three steps. First, we converted postprocessed Sentinel-1 images from SNAP from 32-bit floats to 16-bit integers using the linear method. Next, large images were segmented into 640-pixel patches, generating 1351 patches, and these patches were converted from TIFF to PNG using the GDAL Python package. Finally, the boats in the patches were manually labeled using the LabelImg tool (Tzutalin, 2015) and categorized into 1820 BC, 4306 STB, and 9431 Other. The patch dataset was split into 80 % training and 20 % validation, with batch sizes (16–32) and epochs (100−1000) optimized through fine-tuning. Model performance was assessed via precision, recall, F1 score, mAP@0.50, and mAP@0.50:0.95 (Kumar et al., 2024).

3.4. Estimation of the sand mining volume

After training and validation, the boats were automatically detected from the Sentinel-1 images (2014–2023) using the deep learning model. For sand mining volume estimation, we focused exclusively on the BC type. Each BC was treated as a point, and its coordinates were estimated, following the method detailed in Kumar et al. (2024).

From the BC locations in each image imported into ArcGIS Pro, we determined the sand mining areas for each year by creating polygons covering the BC locations detected throughout the year. Additionally, the average monthly number of BCs at each sand mine was calculated as the average number of BCs detected from satellite images over a month.

The annual sand mining volume at each sand mine was estimated via the following formula:

$$V = \sum_{i=1}^{12} (N_i \text{ x } C \text{ x } t \text{ x } D_i) \quad (1)$$

where V is the total sand mining volume per year at each site, N_i is the average number of BCs in month i at each site, C is the mining capacity of each BC per hour, t is the total mining hours per day, and D_i is the total mining days in month i.

Based on previous studies (Huy, 2017; Ngan, 2023; Truong, 2024; Dang, 2024) and sand mining licenses issued by provincial departments of natural resources and environment (DONRE), the main licensed sand mining boat type in the VMD is the BC, with an operational capacity ranging from 80 to 120 m^3 per hour. The daily mining duration is 10 h (7 AM–5 PM), which is the maximum permitted duration set by Decree No. 23/2020/ND-CP of the Government: Management of riverbed sand and gravel and protection of riverbed, banks, and terraces (Nguyen, 2020). Moreover, in line with the official licensing documents of DONRE (Ngan, 2023; Dang, 2024), we assumed that sand mining activities occurred every day of the month. Finally, we also estimated sand extraction volumes by distributing data across provinces based on administrative boundaries.

The licensed sand extraction volumes in the VMD have been demonstrated to be significantly lower than actual extraction rates in much research, such as Jordan et al., 2019; Lau et al., 2023; Kumar et al., 2024; and Yuen et al., 2024. Therefore, to validate the sand mining volume estimation formula, both its variables and outputs were assessed using a multi-faceted approach. Specifically, the spatial distributions of boats detected from Sentinel-1 imagery were cross-validated using available PlanetScope and Google Earth images for selected dates between 2014 and 2023. These results were further cross-referenced with maps of bathymetric changes in the same period of 2014–2017 and 2017–2020, and the boat counts were compared against those reported in previous studies (Gruel et al., 2022; Lau et al., 2024). In addition, the location of determined sand mines in periods was also compared to the reports on sand mines of DONRE (An Giang and Can Tho). Boat capacities (80–120 m^3/h) were determined using a combination of existing literature and data obtained from DONRE-issued licenses. Sand mining volumes were estimated for three boat capacities (80, 100, and 120 m^3/h) to assess their range. The volume estimated using a 100 m^3/h boat was defined as the base scenario, while the 80 m^3/h and 120 m^3/h capacities, representing a 20 % decrease and increase relative to the base scenario, were used to estimate the potential range of sand mining volumes in the VMD. Moreover, the permitted mining duration was derived from relevant regulatory frameworks and was cross-checked by the field surveys. Finally, the annual estimated sand mining volumes were compared to those reported in prior studies to assess consistency.

3.5. Assessing the impacts of sand mining activity on river morphology using Delft3D

To evaluate the impacts of sand mining activities on sediment dynamics and riverbed morphological changes, a process-based model (Delft3D–FLOW) developed by WL|Delft Hydraulics was established (Deltares, 2024). Delft3D–FLOW was applied for 2–D modeling of hydrodynamic flows and sediment transport in the Bassac River, covering the section from the Chau Doc to Can Tho hydrological stations (Fig. 3a). A curvilinear grid with 20 × 50 m spacing was created for the simulated domain, covering both the rivers and floodplains in the rivers. The grid, consisting of 1764 × 110 cells, was then integrated with river bathymetry to generate a geometric mesh for the model. Model inputs included daily discharge and daily SSC data at the upstream boundaries (Tan Chau and Vam Nao) and daily water levels and SSC data at the downstream boundary (Can Tho).

The riverbed materials consisted of 95 % fine sand with d50 = 214 μm and 5 % mud with d50 = 12.63 μm (Gugliotta et al., 2017). Therefore, only the sand fraction (214 μm) was selected in the simulations, with sediment transport modelled using the van Rijn TR2004 equation

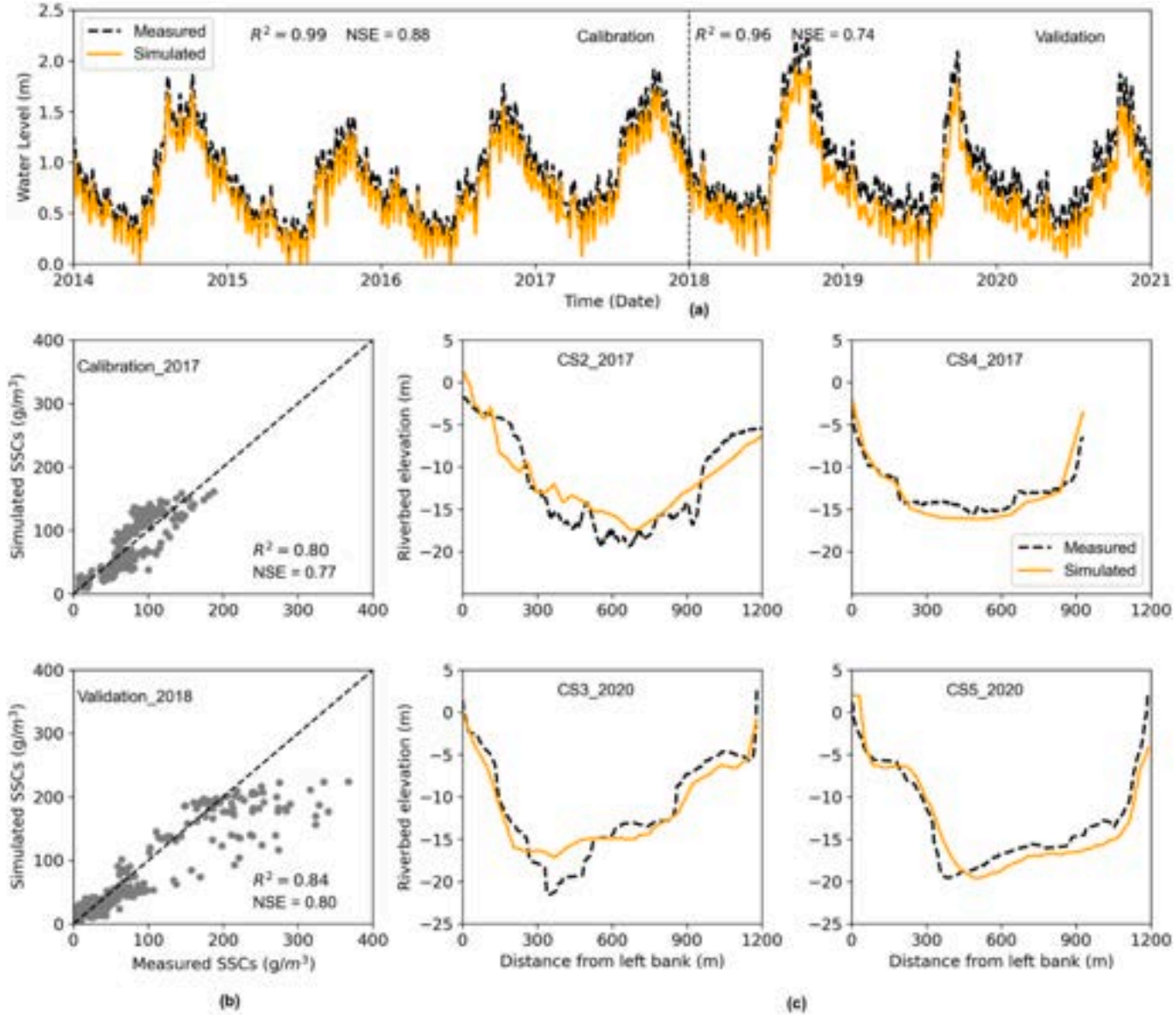

Fig. 7. (a) Simulated and measured water level in 2014–2020 at Long Xuyen station. (b) Simulated and measured SSCs at Thot Not station. (c) Simulated and measured riverbed elevations at four locations (CS2, CS3, CS4, and CS5).

(Jordan et al., 2020). The suspended sediment in the VMD consists primarily of cohesive sediment, which is composed of 1 % sand, 45 % silt, and 54 % clay, with median grain sizes of 10 and 15 μm (Hung et al., 2014; Koehnken, 2014). The Partheniades–Krone formulations were applied for simulating cohesive sediment transport (Jordan et al., 2020). For modeling cohesive sediment dynamics, key parameters include the critical bed shear stress for erosion (τce), erosion rate (M), and settling velocity of sediment (w) for freshwater and for saltwater. The Manning roughness coefficient varied spatially between 0.016 and 0.032 (Thanh et al., 2025).

The simulation of the impact of sand mining in the model was based on depth limits and the daily sand mining volume (Fig. 3). The model automatically calculates the daily mined volume for each location in the mine, following the defined input data. The sand mining areas and volumes were determined in section 3.4 for each year. However, this study simulated the cumulative impact of sand mining over three periods: 2014–2017, 2018–2020, and 2021–2023. For each period, the total area and volume of sand mining were calculated by summing the corresponding annual values. The total sand mining volume for each period was distributed across the total number of mining days, yielding the daily sand mining volume. The mining depth limit was determined based on the average topographic elevation of the sand mining area plus the daily sand mining thickness. The daily sand mining thickness was calculated as the daily sand mining volume divided by the sand mining area. This approach ensured that sediment transport, erosion, and deposition processes were realistically represented across the entire model domain.

The hydrodynamic-sediment transport model was simulated from 2014 to 2023. Since there are no measured discharge data inside this domain, water level data from the Long Xuyen station for 2014–2017 and 2018–2020 were used for model calibration and validation, respectively. The bed elevation and SSCs at the Thot Not in 2017 were utilized for sediment model calibration, whereas the bed elevation in 2020 and SSCs at the Thot Not in 2018 were used for validation. Model performance was evaluated via efficiency indices such as the square correlation coefficient (R^2) and the Nash-Sutcliffe efficiency (NSE).

Three estimates of sand mining volumes were derived from boat capacity scenarios of 80, 100, and 120 m^3/h. The sand mining volume

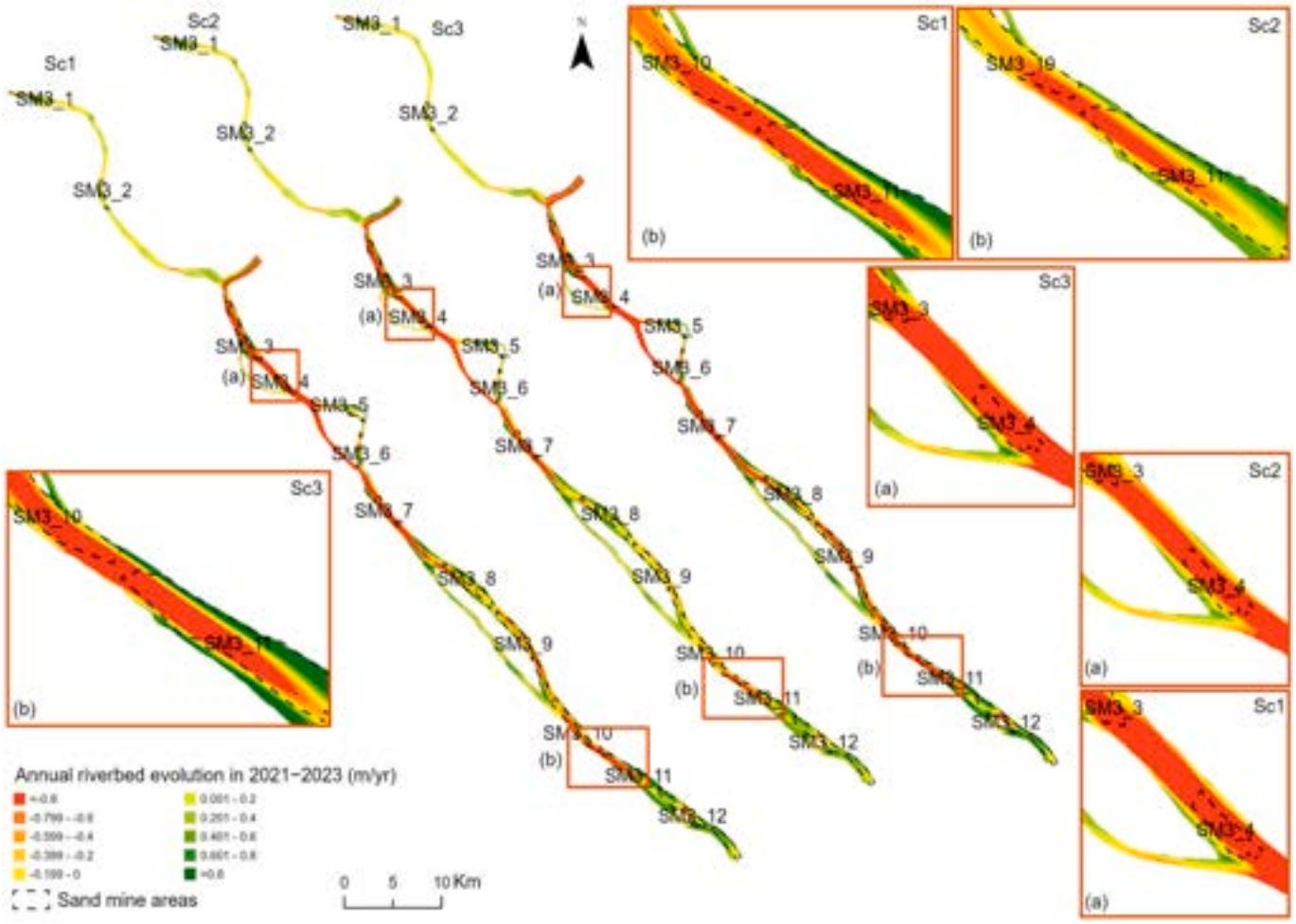

Fig. 8. The annual riverbed evolution in 2021–2023 for three scenarios of Sc1, Sc2 and Sc3. The dotted lines show the limits of mining sites.

estimated from the average capacity (100 m^3/h–Sc1) was used for the calibration and validation of the sediment transport model. The other two scenarios (80 and 120 m^3/h—Sc2 and Sc3, respectively) were applied to further assess the influence of sand extraction intensity on riverbed morphology. These impacts were analyzed through assessments of riverbed evolution, scour hole formation, and thalweg incision and lateral migration over time. Scour holes were identified and classified following Binh et al., 2022, while thalweg incision and lateral migration were quantified by analyzing temporal variations in thalweg elevations and positions across 119 river cross-sections, following Wen et al. (2025).

4. Results

4.1. Boat detection performance of the YOLO model

This study evaluates the performance of the YOLOv5 deep learning model in detecting three boat categories—BC, STB, and Other—across different batch sizes. Fig. 4 presents key performance indicators, including loss curves and model accuracy trends for various batch sizes, a confusion matrix, and precision-recall and precision-confidence curves for each category. These visualizations comprehensively assess the model's efficiency in small boat detection. Table 2 details the model's performance on validation data for batch size 32.

The loss curves illustrate box loss, objectness loss, and classification loss for training and validation across 16, 25, and 32 batch sizes (Fig. 4a). A steep decline in loss values is initially observed, indicating rapid feature learning. After approximately 400 epochs, the loss stabilizes, suggesting model convergence. A batch size of 32 consistently results in the lowest loss values, particularly for the validation box loss and classification loss. This suggests that a larger batch size contributes to improved learning efficiency and generalizability compared to smaller batch sizes. This trend is further confirmed by model performance metrics, where a batch size of 32 outperforms the other sizes (Fig. 4b).

The confusion matrix shows a classification accuracy of 91 % for BC, 87 % for STB, and 84 % for Other for batch size 32, with minor misclassifications, mainly between BC and STB, suggesting feature overlap. Moreover, for the BC detection with this batch, the mAP@0.5 reaches 0.958, with an mAP@0.5_0.95 of 0.66, demonstrating high reliability (Table 2). These results align with benchmarks (> 0.5) set by Ultralytics (2022), validating the model's effectiveness in small boat detection. Additionally, as shown in Fig. 5, the deep learning model detected boats with high confidence scores. With a batch size of 32, the model achieved a mean confidence score of 0.815 for the BC detection in 2014–2023. The standard error was calculated as 0.0031, leading to a 95 % confidence interval ranging from 0.809 to 0.821. This narrow interval indicates a highly consistent and statistically reliable confidence in BC detections, suggesting that the model's predictions for this boat type are robust.

4.2. Sand mining volume estimation

From October 2014 to December 2023, the YOLOv5l model detected

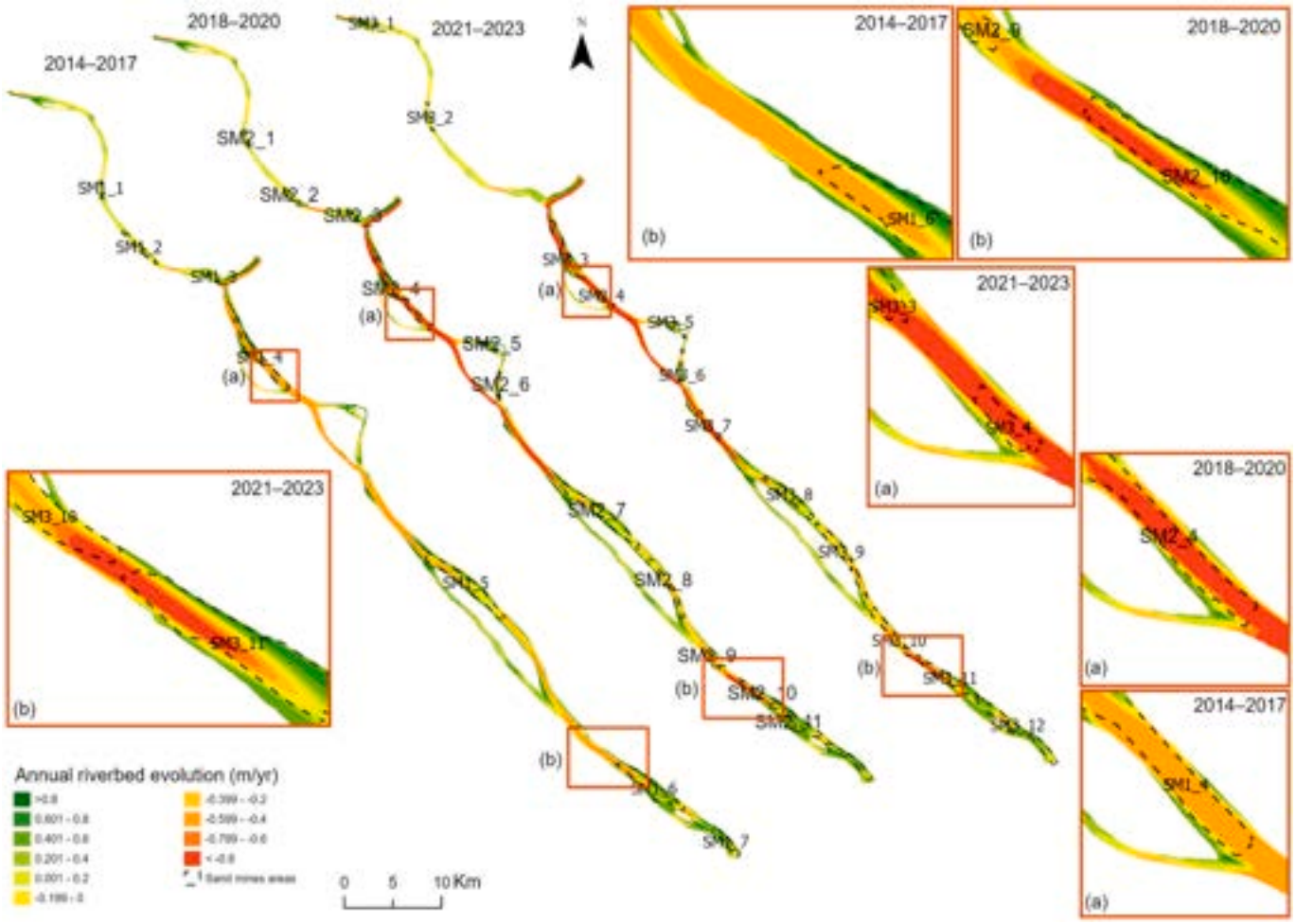

Fig. 9. The annual riverbed evolution in Sc2 in three periods: 2014–2017, 2018–2020, and 2021–2023. The dotted lines show the limits of mining sites.

67,401 boats from 635 Sentinel-1 images. Among these, BCs accounted for 12.7 % (8560 boats), whereas the STBs accounted for 26.7 % (17,982 boats). The remaining boats (60.6 %) were classified as the Others. The number of STBs was approximately twice that of BCs, primarily due to clustering 1–3 STBs with a single BC at extraction sites for sand transport to other locations (Kumar et al., 2024).

Over the same period, 386 BCs were recorded in the Bassac River. The annual number of BCs increased significantly from 30 in 2014 to 51 in 2019 before decreasing to 37 boats in 2023 along the Bassac River (Fig. 6a and Table S1). The highest concentration of BCs was in An Giang, where 143 boats (37 %) were recorded between 2014 and 2023, with 2023 having the highest number at 24 boats. Boat activity varies considerably by month, aligns with seasonal hydrological patterns, peaks in the dry season (January–June), and decreases during the flood season (July–December).

The total sand extraction volume between 2014 and 2023 from the Bassac River was estimated at 92.68 Mm^3, 116.04 Mm^3, and 137.59 Mm^3, corresponding to boat capacity scenarios of 80, 100, and 120 m^3/h, respectively. This result indicates that varying boat capacity within 80–120 m^3/h changed the total sand mining volume by about ±20 % from the baseline assumption of 100 m^3/h. Under the baseline scenario, the average annual extraction volume was 12.54 ± 2.51 Mm^3 during 2014–2023. The annual extraction volume increased from 9.86 ± 1.97 Mm^3 in 2015 to a peak of 16.15 ± 3.23 Mm^3 in 2019 before declining to 11.99 ± 2.40 Mm^3 in 2023 (Fig. 6b and Table S2).

Sand mining activities in the Bassac River occurred across multiple provinces, including An Giang (AG), Dong Thap (DT), Can Tho (CT), Vinh Long (VL), Hau Giang (HG), Soc Trang (ST), and Tra Vinh (TV) (Fig. 6c and Figs. S1a and S2a). Three provinces, An Giang, Can Tho, and Vinh Long, accounted for the highest extraction volumes, exceeding a total volume of 20 Mm^3 each and collectively making up 74.3 % of the total sand mined in 2014–2023. An Giang recorded the highest extraction volume at 37.04 ± 7.41 Mm^3 (31.9 % of the total), whereas Hau Giang had the lowest at just 2.2 %. An Giang remained the most active province in sand mining, reaching its annual extraction volume peak of 6.0 ± 1.21 Mm^3 in 2022. Vinh Long recorded the highest annual extraction volumes in 2017 (2.89 ± 0.58 Mm^3) and 2019 (4.48 ± 0.90 Mm^3), whereas Can Tho peaked in 2018 at 2.97 ± 0.59 Mm^3 (Tables S3–5).

A total of 152 sand mines were identified in the Bassac River from 2014 to 2023. The number of sand mines increased from 14 sites in 2014 to a peak of 20 sites in 2019 before declining to 14 sites in 2023. The annual extraction volume of sand mines varied widely, with the lowest recorded value of 0.08 ± 0.02 Mm^3/yr in 2014 and the highest recorded value of 3.42 ± 0.68 Mm^3/yr in 2023 (Fig. 6d). For modeling purposes, sand mining activities were analyzed across three periods: 2014–2017, 2018–2020, and 2021–2023. The number of sand mines increased from seven in 2014–2017 to eleven in 2018–2020 and twelve in 2021–2023. The sand extraction volume of the sand mines during these periods ranged from 0.12 ± 0.02 Mm^3/period to 10.85 ± 2.17 Mm^3/period. The total daily sand volume per mine fluctuated, with a minimum of 991.87 ± 198.37 m^3/day during 2014–2017 and a maximum of 9905.78 ± 1981.16 m^3/day during 2018–2020. A detailed breakdown of the sand extraction volumes for each period is provided in Table 3 and

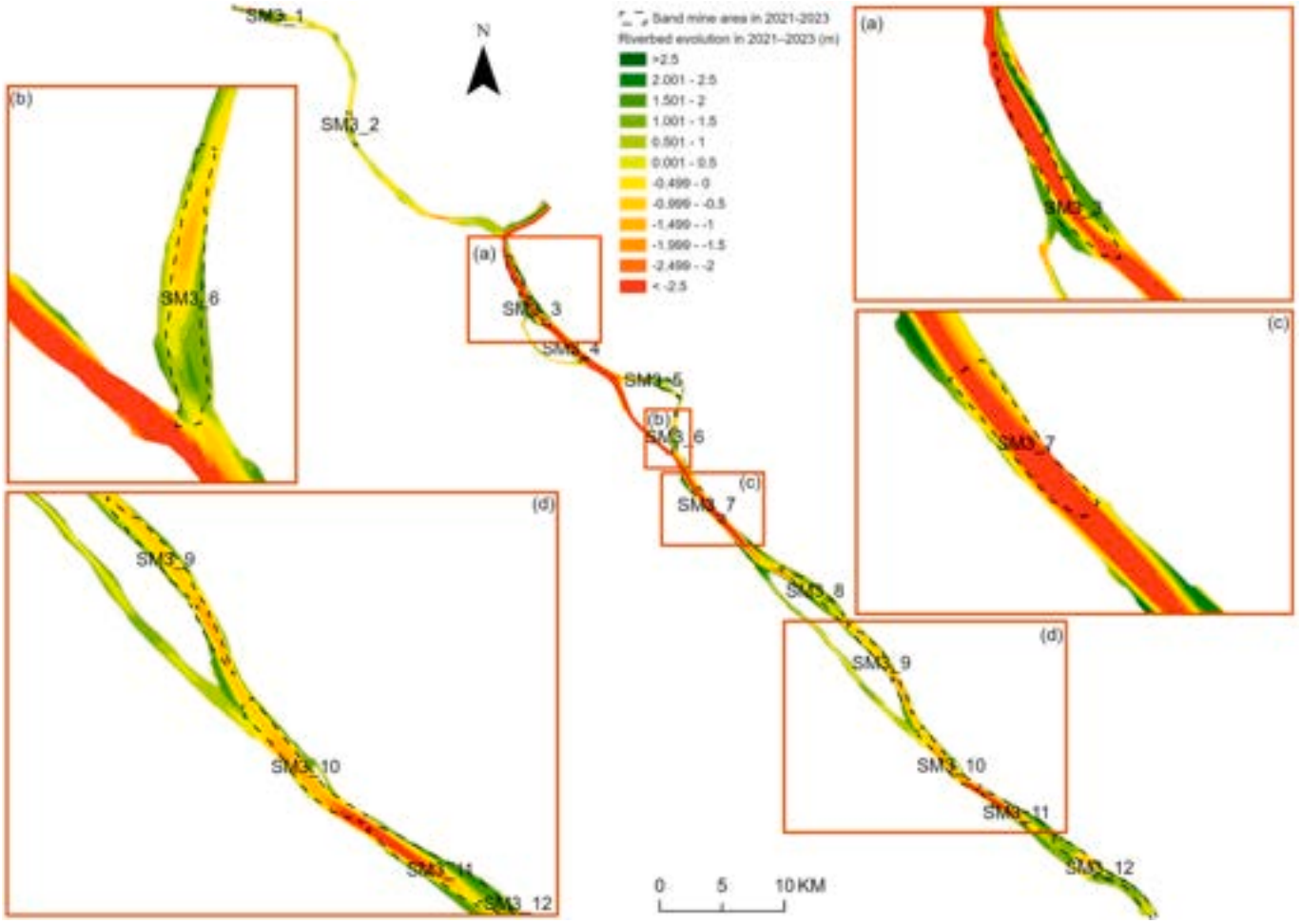

Fig. 10. The simulated erosion and sedimentation depth in the Bassac River at the sand mines in 2021–2023 in Sc2. The dotted lines show the limits of mining sites.

Tables S6–7.

4.3. Impacts of sand mining on riverbed morphology

4.3.1. Calibration and validation results of the Delft3D model

Sixty-four trials were simulated to optimize the parameters of the hydro sediment-morphodynamics model. Fig. 7 presents the simulated and observed data and the best parameter values during the calibration and validation periods. The model effectively simulated water levels at the Long Xuyen station (Fig. 7a), achieving high R^2 values (0.96–0.99) and NSE coefficients (0.74–0.88), indicating a strong fit. The sediment concentration simulations also performed well despite the limited observed data. At the Thot Not location, the R^2 coefficients were notably high during calibration (0.80) and validation (0.84), while the NSE coefficients for the SSC simulations were 0.77 and 0.80, respectively (Fig. 7b). Additionally, the model successfully captured riverbed elevation changes in 2017 and 2020 (Fig. 7c). These results confirm strong agreement between the simulated and observed data during both the calibration and validation phases, verifying the model's ability to assess anthropogenic impacts on river flow and geomorphology. This ensures its reliability for regional evaluations.

4.3.2. Morphological changes under the impacts of sand mining activities

4.3.2.1. Spatiotemporal variability in riverbed evolution. Fig. 8 shows the annual riverbed evolution of the Bassac River in 2021–2023 for the Sc1, Sc2, and Sc3, and Fig. S3 and Fig. 9 show the annual riverbed evolution in the Sc1 and Sc2 over three periods, respectively, namely, 2014–2017, 2018–2020, and 2021–2023, under the impacts of sand mining.

The total net incision volumes from 2014 to 2023 were −141.14 and −239.01 Mm^3 in scenarios Sc2 and Sc3, respectively, representing a 25 % decrease and a 27 % increase compared to Sc1 (−188.19 Mm^3). On average, the mean annual riverbed incision of the Bassac River in 2014–2023 decreased by 21.9 % in Sc2 (−0.52 m/yr) and increased by 23.7 % in Sc3 (−0.82 m/yr), relative to Sc1 (−0.66 m/yr). The mean annual incision rates in Sc1 were −0.56, −0.62, and −0.81 m/yr in 2014–2017, 2018–2020, and 2021–2023, respectively. The corresponding values were −0.41, −0.48, and −0.66 m/yr in Sc2 and −0.67, −0.80, and −0.98 m/yr in Sc3. We estimated that the net annual incision volume in Sc1 increased from −14.93 Mm^3/yr in 2014–2017 to −23.21 Mm^3/yr in 2021–2023. A similar trend was observed in Sc2, with values of −11.20 and −17.41 Mm^3/yr, and in Sc3, with values of −18.96 and −29.48 Mm^3/yr.

The simulation results underscore the spatial variability in riverbed evolution along the Bassac River. Erosion was more pronounced in the lower section, from the Vam Nao River confluence to the Can Tho station, than in the upper section, which extends from the Chau Doc station to the Vam Nao confluence. This contrasting pattern is largely attributed to the concentration of sand mining activities and flow in the lower reach. Between 2014 and 2017, the net annual incision volume in the upper section accounted for 8.4 % (−0.94 Mm^3/yr) in Sc2 to 10.3 % (−1.95 Mm^3/yr) in Sc3 of the total net incision volume of the entire river reach. This share increased to 12.6 % (−2.19 Mm^3/yr) in Sc2 and 16.9 % (−4.98 Mm^3/yr) in Sc3 in 2021–2023. Conversely, the contribution of the lower section to the total net incision volume in three scenarios accounted for a large percentage, from 83.1 % to 91.6 %, in 2014–2023.

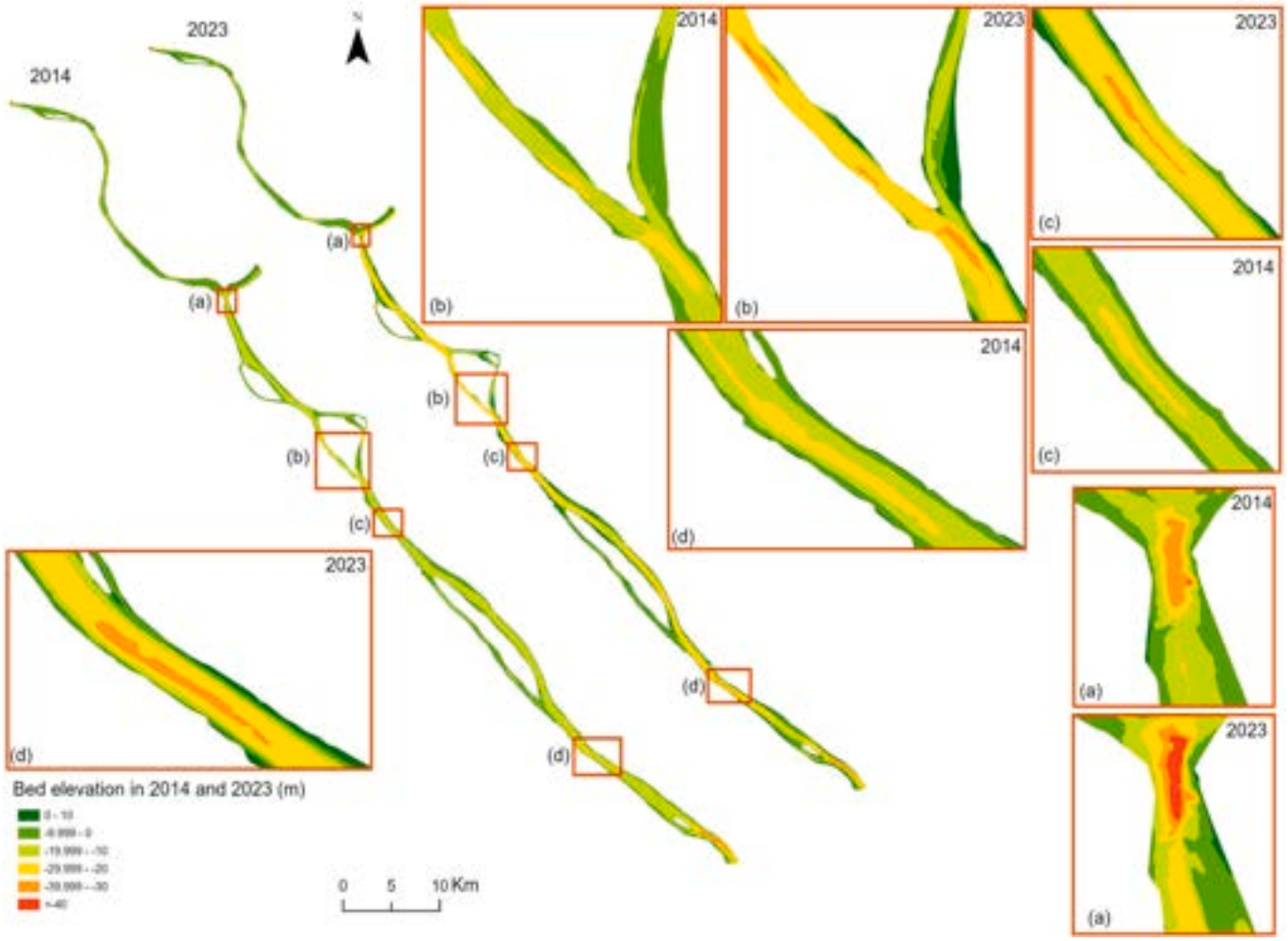

Fig. 11. The riverbed elevation in the Bassac River in 2014 and 2023 in Sc1.

The mean net incision rate in 2014–2023 was −0.24, −0.18, and − 0.45 m/yr in the upper section, whereas it was −0.65, −0.57, and −0.85 m/yr in the lower section for Sc1, Sc2, and Sc3, respectively, reflecting intensified erosion dynamics downstream.

Sand mining activities have significantly altered riverbed elevations around mining sites. Figs. S4–6 and Fig. 10 provide an overview of riverbed evolution with the sand mining sites in the Bassac River in Sc1 and Sc2 in 2014–2017, 2018–2020, and 2021–2023, respectively. Both sedimentation and erosion occur simultaneously at sand mining locations, although erosion is more pronounced downstream of the mining sites. The impacts of erosion associated with a sequence of sand mining sites extend up to 10 km upstream and downstream.

4.3.2.2. Scour hole formation under the impact of sand mining. According to Figs. 11 and 12, the model predicted the formation of twenty-three scour holes in the Bassac River between 2014 and 2023 in Sc1. Following the classification method of Binh et al., 2022, riverbed scour holes are divided into three different categories: shallow (<5 m), medium (5–10 m), and deep (>10 m). Based on this classification, eight scour holes were identified as shallow, whereas the remaining were classified as medium in Sc1. In Sc2 and Sc3, the locations and total number of scour holes were consistent with Sc1. However, the depth distribution differed: in Sc2, twelve scour holes were shallow and eleven were medium, whereas in Sc3, seven were shallow, five were medium, and eleven were deep. By 2023, the maximum scour depths reached −9.0 m in Sc1, −7.5 m in Sc2, and −11.0 m in Sc3. The most severe scour holes were predominantly associated with sand mining sites, whereas the others were primarily located at river confluences and meandering sections.

4.3.2.3. Spatiotemporal variability in river thalweg. Fig. 13 illustrates the thalweg and cross-sectional riverbed elevation along the Bassac River in Sc1 from 2014 to 2023. Under the Sc1, the river thalweg in the Bassac River experienced substantial incision, with a mean value of −3.56 m during 2014–2017, corresponding to an annual incision rate of −0.89 m/yr. The mean river thalweg incision decreased 26.4 % in 2017–2020 (−2.62 m) and 18.7 % in 2020–2023 (−3.0 m), equivalent to incision rates of −0.87 m/yr and −1.0 m/yr, respectively, compared to 2014–2017. Over the 2014–2023 period, the mean thalweg incision was −9.18 m, with a mean annual rate of −0.92 m/yr. Most incision occurred at the river section between the Vam Nao confluence and Can Tho station, with a mean of −8.62 m, compared to −1.48 m in the remaining sections. In addition, severe incision was primarily observed in meandering segments and confluence upstream and downstream of an island. Compared to Sc1, the mean thalweg incision rate decreased 24.8 % (−0.69 m/yr) in Sc2 and increased 28.3 % (−1.18 m/yr) in Sc3 during 2014–2023.

The thalweg migration distances also varied markedly over the study period (Fig. 14). From 2014 to 2017, the migration distance ranged from 3.28 to 296.6 m, with an average of 52.5 m. In this period, 87 % of migration distances were < 100 m, 7.8 % ranged from 100 to 200 m, and the remaining 5.2 % were between 200 and 300 m. Compared to 2014–2017, the maximum migration distance increased by 19.9 % (355.54 m) in 2017–2020 and 36.8 % (405.73 m) in 2020–2023, while

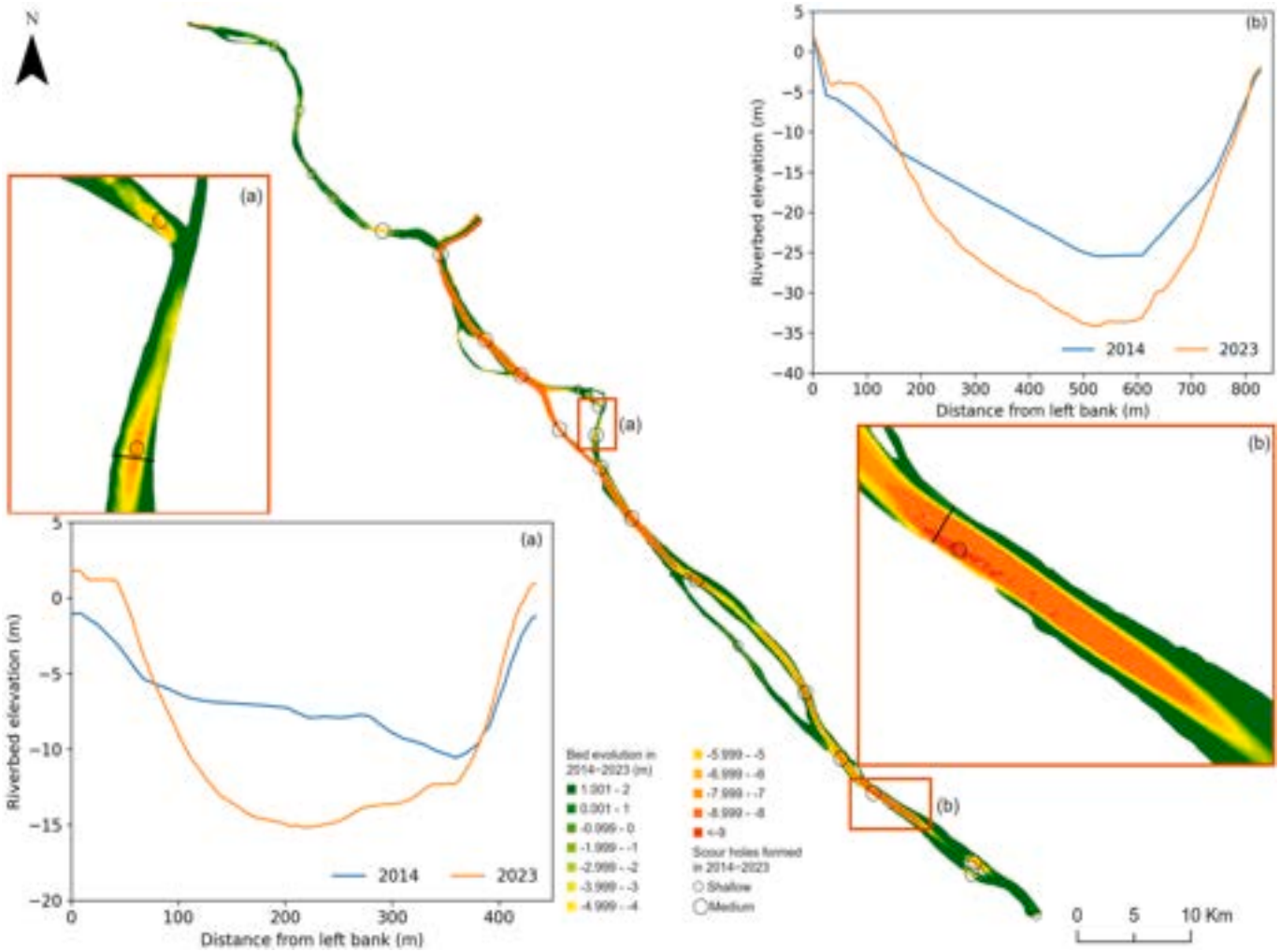

Fig. 12. The riverbed evolution in the Bassac River with typical locations (at scour holes) in 2014–2023 in Sc1. Twenty-three scour holes (indicated by black circles) are formed.

the mean distances increased by 17.7 % (61.83 m) and 75.9 % (92.33 m), respectively. However, the proportion of migration distance < 100 m decreased by 5.2 % and 7.8 % in 2017–2020 and 2020–2023, respectively, compared to 2014–2017. The period 2020–2023 exhibited the highest migration distance, reaching up to 405.73 m, with 0.9 % of migration distance > 400 m. Overall, the migration distance on average in 2014–2023 was 98.30 m, with a maximum of 478 m. During this period, 79.1 % of migration distances were less than 100 m, and 2.6 % exceeded 400 m. Compared to Sc1, the mean migration distances were decreased 15 % in Sc2 (83.56 m) and increased 18 % in Sc3 (116 m) during 2014–2023.

5. Discussion

5.1. Sand mining boat number and locations

Our study estimated a total of 386 BCs in the Bassac River from 2014 to 2023, with an average of 38.6 boats per year. Using data from Gruel et al. (2022), Lau et al. (2024) estimated 344 BCs in the Bassac River between 2014 and 2020, with an average of 49.1 boats per year. The discrepancy in boat counts is primarily due to differences in detection methods.

In the study of Gruel et al. (2022), the authors classified BCs solely by size, considering only those longer than 70 m via Sentinel-1 imagery. As a result, certain boat types with lengths > 70 m, such as cargo ships, may have been misclassified or included, particularly in regions of the VMD with high port activity. However, both studies revealed that Can Tho was a hotspot for sand mining activity in the Bassac River. Our findings were further validated by comparing boat locations with bathymetric changes in 2014–2017 and 2017–2020. As shown in Fig. 15, there is a clear correlation between the locations of the sand mining boats and the erosion areas during 2017–2020. In addition, the location of sand mines in the periods was also validated by the reports on sand mines of DONRE (An Giang and Can Tho).

5.2. Sand mining volume comparison analysis

Several studies have estimated sand mining volumes by using different methods in the VMD from 2014 to 2023. Notable examples include Eslami et al. (2019), who analyzed statistical reports on sand mining licenses, as well as Gruel et al. (2022) and Kumar et al. (2024), who estimated extraction volumes by correlating boat density maps with bathymetric differences. On the basis of reported licenses, Eslami et al. (2019) estimated that 28 Mm^3 of sand was extracted from the VMD in 2015, with the Bassac River accounting for 32.1 % (9 Mm^3) of this total. In comparison, our study estimated an extraction volume of 7.83–11.75 Mm^3 from the Bassac River in 2015, representing values 13 % lower to 30.6 % higher than the estimate of Eslami et al. (2019). Nevertheless, their estimate falls within the range derived in this study, and the volume estimated under an assumed mining capacity of 100 m^3/h (9.85

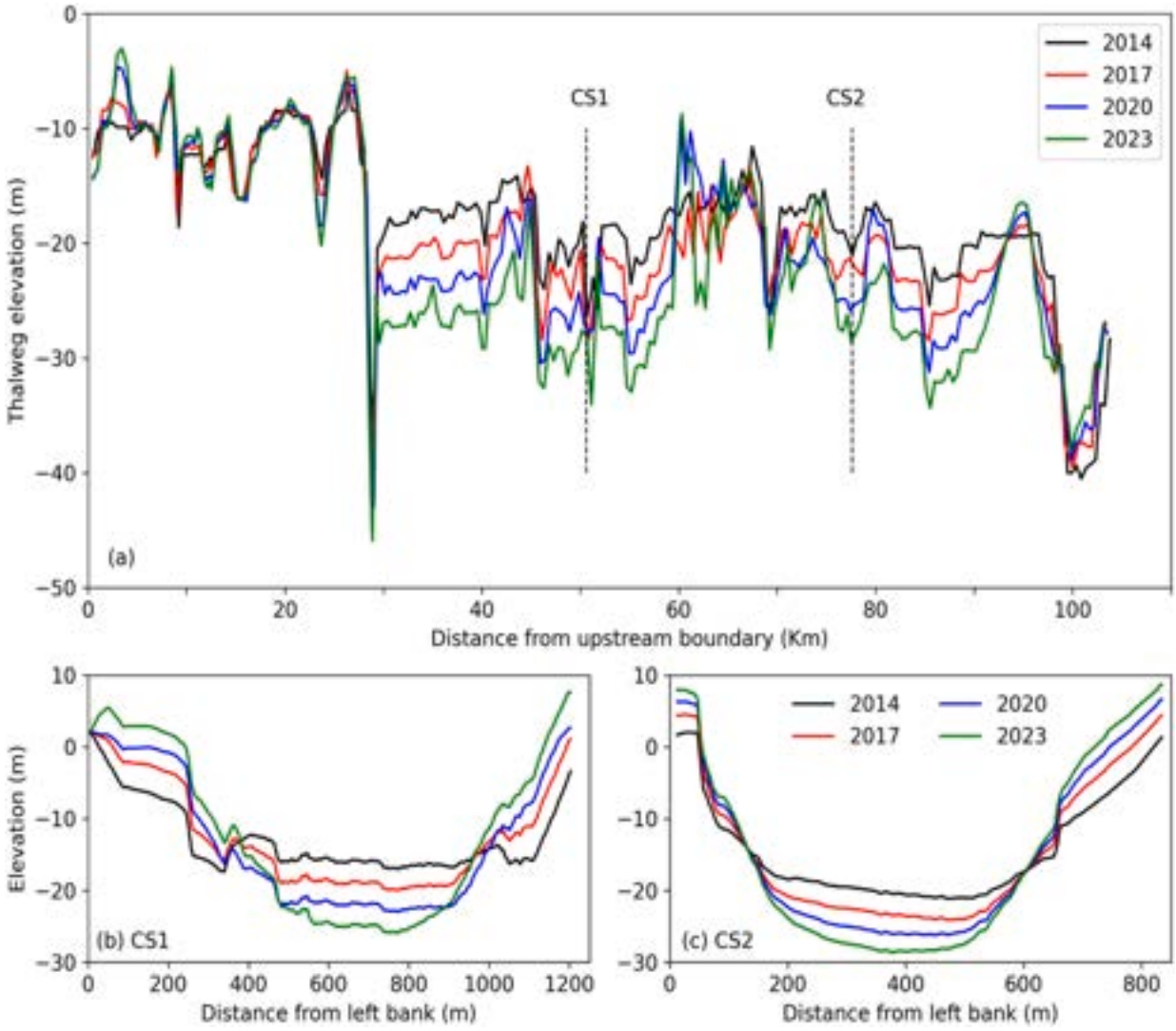

Fig. 13. (a) Thalweg elevation along the Bassac River from Chau Doc station to the Can Tho station in 2014–2023 in Sc1, (b) Elevation of cross-section CS1, (c) Elevation of cross- section CS2.

Mm^3) deviates by only 9 % from the value reported by Eslami et al. (2019).

More recently, Gruel et al. (2022) and Kumar et al. (2024) applied the same method of correlating boat density maps with bathymetric differences (2014–2017) to estimate sand extraction volumes. Figs. 16a and b compare the sand mining volumes estimated in our study with those reported by Gruel et al. (2022) and Kumar et al. (2024). According to Gruel et al. (2022), sand extraction from the Bassac River ranged from 7.3 Mm^3/yr in 2015 to 7.9 Mm^3/yr in 2020, with a total volume of 44.2 Mm^3. In addition, Kumar et al. (2024) further estimated extraction volumes for three provinces (Can Tho, Hau Giang, and Soc Trang), from 2.86 Mm^3 in 2015 to 4.26 Mm^3 in 2022. In contrast, our results for three different boat mining capacities indicate extraction volumes were 1.07 to 2.45 times greater than those reported by Gruel et al. (2022) and 0.8 to 1.5 times greater than those reported by Kumar et al. (2024) during the same timeframe. Both Gruel et al. (2022) and Kumar et al. (2024) indirectly estimated extraction volumes in the Bassac River using a correlation formula derived from bathymetric differences and boat density in 2014–2017 in the Mekong River, while our approach directly estimated volumes based on boat mining capacity and locations in the Bassac River. This methodological difference largely explains the discrepancy in estimated extraction volumes among the three studies. It should be noted that the sand mining volumes estimated in our study represent the maximum extraction capacity of the sites per year. This is because our calculation assumed an exploitation time of 10 h per day, as specified by Decree No. 23/2020/ND-CP of the Government: Management of riverbed sand and gravel and protection of riverbed, banks, and terraces (Nguyen, 2020). In practice, however, field observations indicate that BCs operated within the prescribed time frame but often paused operations when sand transport boats (STBs) entered and exited to collect sand, which meant the actual exploitation time was lower. Another factor affecting mining duration is the number of active mining days per month. While official licensing documents often assume continuous operation and calculate authorized extraction volumes accordingly (Ngan, 2023; Dang, 2024), actual mining days may be fewer due to equipment failures or adverse weather. As Sentinel imagery does not provide complete daily coverage to accurately determine the number of mining days, we assumed that sand mining activities occurred every day of the month. Nonetheless, our estimates using the boat mining capacity of 100 m^3/h align closely with those of Kumar et al. (2024), with an RMSE of 0.4 Mm^3/yr and a PBIAS of 8 % when comparing sand mining volumes for the three provinces from 2015 to 2022 (Fig. 16b).

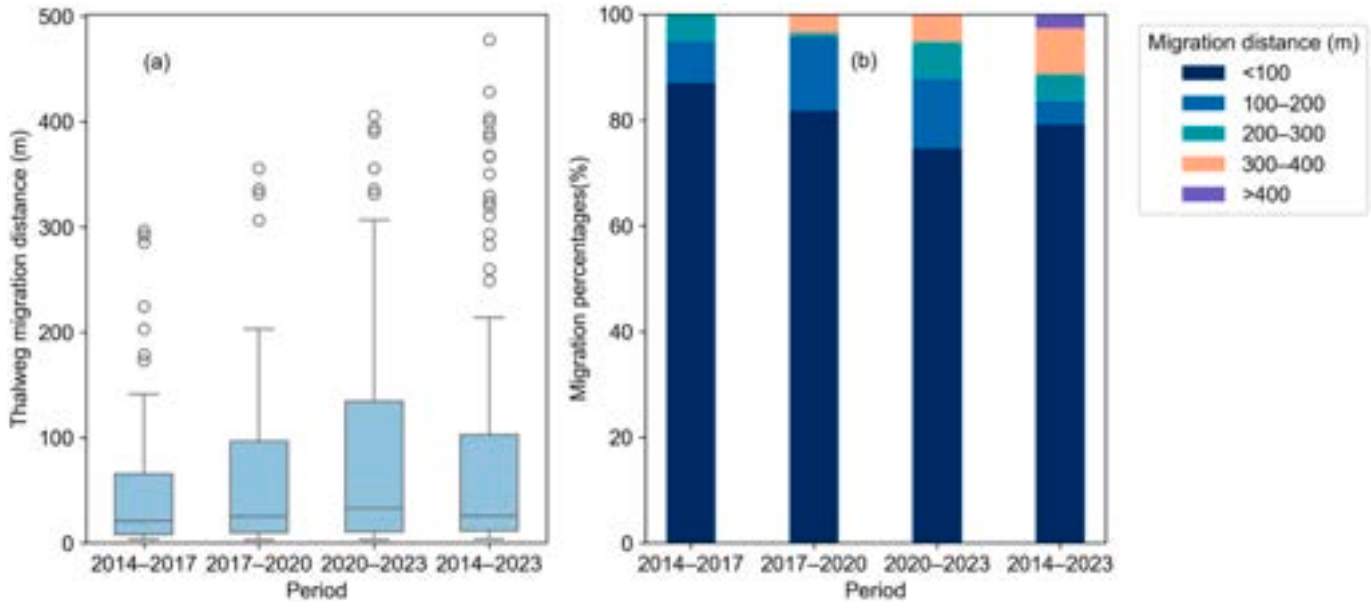

Fig. 14. (a) Thalweg migration distance and (b) migration percentages along the Bassac River from Chau Doc station to the Can Tho station in the periods of 2014–2023 in Sc1.

5.3. Morphological changes under the impact of sand mining activities

We simulated the sediment transport process and assessed the impact of sand mining on river morphology in the Bassac River from 2014 to 2023 by using modeling techniques. By comparing bathymetric data from different years (2005, 2017, 2020), Ahmed et al. (2025) estimated that the river reach from Chau Doc to Can Tho experienced an annual net riverbed incision volume of −16 Mm^3/yr between 2005 and 2017 and −20.5 Mm^3/yr from 2017 to 2020. Our estimations of the net annual riverbed incision volume were 30 % lower to 18.5 % higher in 2014–2017 and 28.3 % lower to 21.4 % higher in 2018–2020 than the results of Ahmed et al. (2025). Additionally, Lau et al. (2023) reported that the Bassac River lost 31.8 Mm^3/yr in 2017–2020, equating to 47 % of the riverbed being incised from Chau Doc to Can Tho, whereas Ahmed et al. (2025) reported a 53 % incision rate during the same period. In contrast, our study revealed an incision rate ranging from 43.1 % to 55.1 %, with a volume loss of 27.9 to 47.2 Mm^3/yr in 2018–2020. Nonetheless, their reported values fall within our estimated range, with only a 2.1–3.9 % difference, and our findings of Sc1 (51.3 %) closely align with those of Ahmed et al. (2025).

Additionally, sand mining volumes increased from 5.19–7.78 Mm^3/yr in 2014–2017 to 9.82–14.72 Mm^3/yr in 2021–2023 in the upper Bassac River (Chau Doc to Can Tho). By the method of Zhang et al. (2022) and Ahmed et al. (2025), a comparison of these values with the total annual net riverbed changes revealed that the sand mining accounted for 41.0–46.3 % of total riverbed incision during 2014–2017, rising to 49.9–56.4 % during 2021–2023. The growing contribution of sand mining to riverbed erosion over time results from rising extraction volumes driven by construction demands, as shown in Fig. 17, which illustrates a moderate positive correlation between annual sand mining volume and annual riverbed incision volume from 2014 to 2023. Our estimates exceed those reported by Ahmed et al. (2025) and Binh et al., 2021. Ahmed et al. (2025) estimated sand mining contributions of 27.72 % in 2005–2017 and 35.3 % in 2017–2020 in the VMD, whereas Binh et al., 2021 reported contributions of 23.4 % in 1998–2014 and 25.6 % in 2014–2017 for the Mekong River from Tan Chau to My Thuan. However, these studies relied on licensed sand extraction volumes, which have been demonstrated to be significantly lower than actual extraction rates (Lau et al., 2023; Kumar et al., 2024; Yuen et al., 2024). Moreover, it should be noted that the sand mining impact values we calculated represent the maximum possible contribution to riverbed incision in the Bassac River, since the sand mining volumes used correspond to the maximum extraction capacity of the sites per year.

Furthermore, Kim et al. (2025) applied the MIKE 21FM model to simulate the impacts of sand mining on river morphology. Their study revealed that the operation of 26 sand mines along the Mekong River (from Tan Chau to My Thuan) led to the highest recorded erosion rates of −1.21 m/yr in the Mekong River and −0.5 m/yr in the Bassac River in 2017. Our analysis revealed a different incision rate of −0.41 to −0.67 m/yr in 2014–2017 in the Bassac River, possibly because our study directly simulated the impact of sand mining on the Bassac River, whereas Kim et al. (2025) assessed the indirect effects of sand mining in the Mekong River.

Finally, we found that sand mining has a pronounced impact on riverbed incisions in upstream and downstream areas, extending up to 10 km from the sequence of sand extraction sites in the Bassac River. These findings align with those of Kim et al. (2025) and Kondolf (1997). Moreover, under the impact of sand mining, twenty-three scour holes with depths of up to 11 m formed between 2014 and 2023. In addition, the thalwegs of the Bassac River were incised with a mean rate of up to −1.18 m/yr. We also found that the thalweg migrated during 2014–2023, with an average migration distance of 98.30 m and a maximum of 478 m. Most scour holes and severe thalweg incisions developed at the sand mining sites, the river confluences, and meandering segments. Despite variations in scour hole formation processes across geomorphological contexts (Ferrarin et al., 2018), the common mechanism was the high erosive capacity of flow within the scour holes, caused by elevated flow velocity and bed shear stresses (Binh et al., 2022). This, combined with the thalweg migration toward riverbanks, contributed to bank instability and collapse. Notably, the locations of riverbank erosion reported by Vu et al. (2024) closely match the locations of scour holes identified in our study. This is also consistent with the conclusion of Binh et al. (2022) that scour holes are one of the main drivers of riverbank erosion in the VMD.

5.4. Integration of methods for river management

The integration of deep learning, remote sensing, and numerical modeling was applied in this study to enhance river management. Specifically, the synergy between YOLO-based object detection and

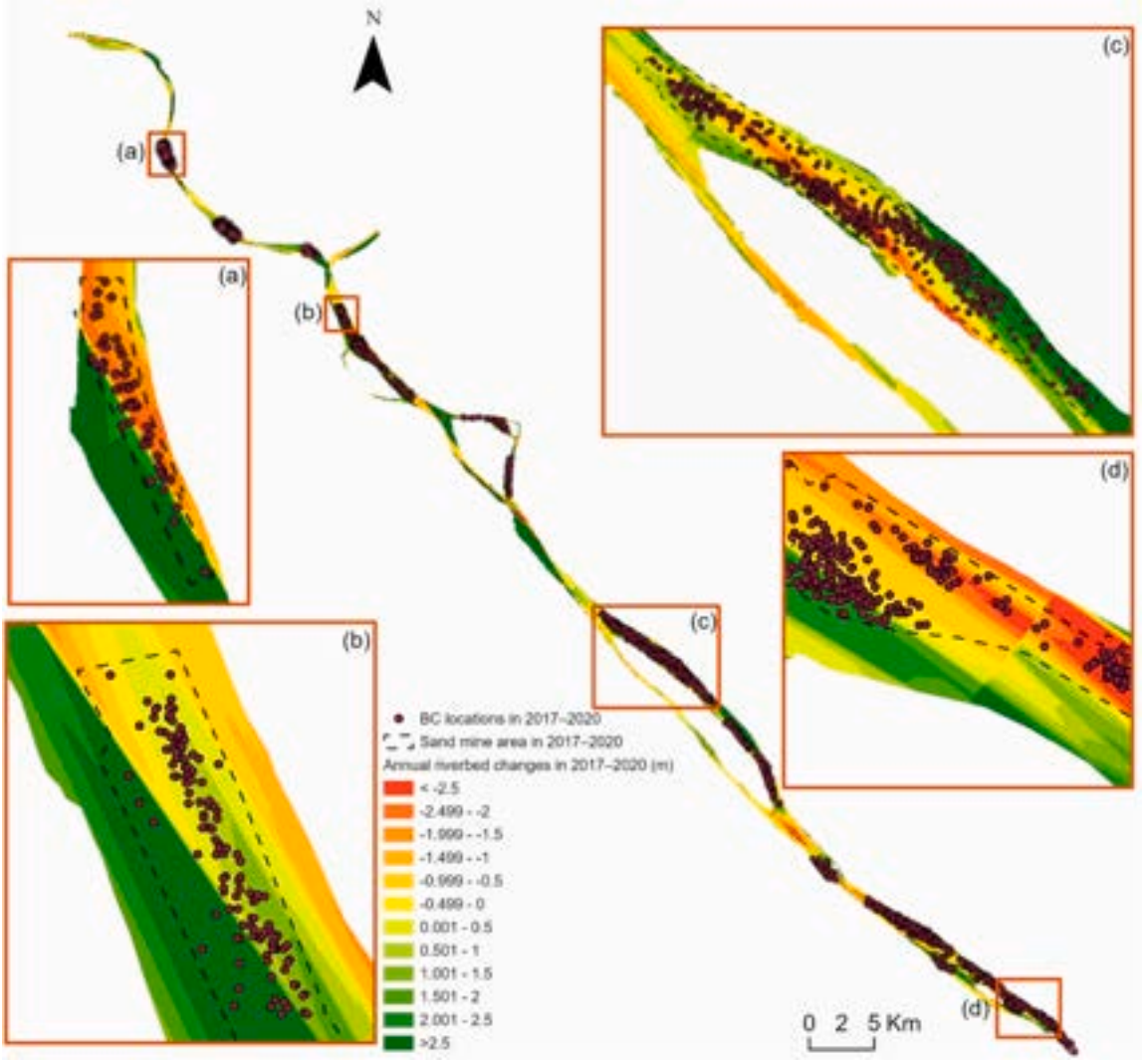

Fig. 15. Annual riverbed changes in the Bassac River in 2017–2020, including the spatial locations of the BCs and the sand mine areas in the same period.

Delft3D modeling is crucial in this approach. YOLO enables real-time detection of sand mining activities from remote sensing imagery, providing spatial and temporal insights into extraction patterns. Unlike previous studies, such as Kumar et al. (2024), who indirectly estimated sand mining volumes in the Bassac River by correlating boat density maps with bathymetric difference maps (2014–2017) in the Mekong River, our method directly determined extraction volumes based on boat mining capacity and locations in the Bassac River. Moreover, their analyses assumed that all bathymetric differences were solely the result of sand mining, overlooking the influence of other potential factors. One advantage of our method is that it uses a single formula to estimate sand mining volumes with the validated variables, and it does not rely on bathymetric data, which is often unavailable for many rivers. This makes our approach more adaptable and applicable to other river systems where sand mining is a concern but field measurements are limited.

Furthermore, the estimated sand mining volumes for mining areas serve as crucial inputs for hydraulic and sediment transport modeling, which simulates hydrodynamic and morphological changes in river systems. Moreover, applying the dredging and mining module to model the impact of sand mining based on daily extraction volumes further enhances the reliability of river morphology simulations. By integrating these techniques, our method enhances the accuracy of sand mining volume estimation and improves the assessment of its environmental impacts, ultimately supporting sustainable river management strategies. This method can be readily applied to other river systems facing similar challenges related to sand mining.

5.5. Limitations and outlook

Despite its advantages, this approach has certain limitations. First, applying the deep learning model to detect BC boats still involves uncertainties. Although the model demonstrated high performance, with most indicators exceeding 0.8, certain errors in boat type classification persist, particularly misclassification between STB and BC boats (8 %). However, given the large study area and the substantial number of detected BC boats, this error is relatively minor and acceptable. Future improvements could focus on optimizing the learning algorithm and expanding the training dataset to increase accuracy. Second, using Sentinel-1 images presents another limitation due to their grayscale color band and 10-m resolution. Nevertheless, these data remain the highest available frequency and resolution and freely accessible data for the VMD, while higher-resolution imagery (e.g., PlanetScope, 2–3 m) is costly or weather-dependent, limiting its applicability for large-scale, continuous monitoring. Third, BCs in the VMD have mining capacities of 80–120 m^3/h (Huy, 2017; Ngan, 2023; Truong, 2024; Dang, 2024). Because detailed capacity data for individual boats were unavailable, we used an average value for all BCs corresponding to each capacity level. However, our estimates provided a range that covers both the minimum

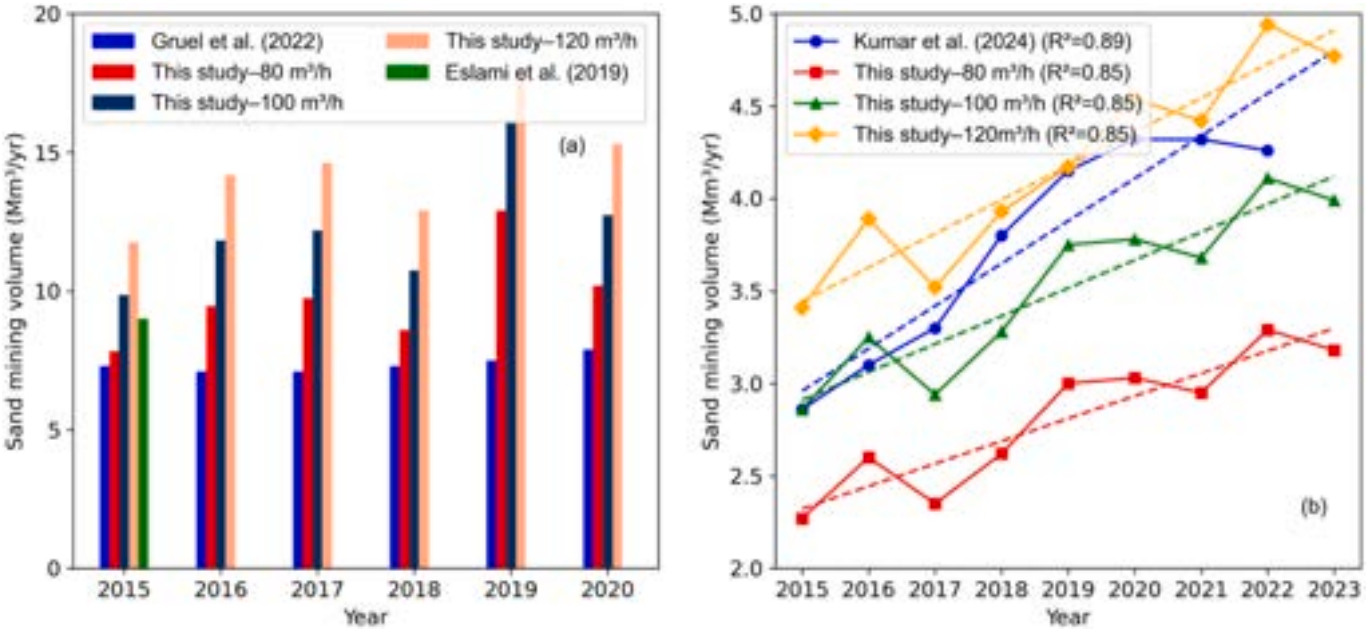

Fig. 16. Comparison of the annual total sand mining volume: (a) In the period of 2015–2020 for the Bassac River with the research of Eslami et al. (2019) and Gruel et al. (2022). (b) In the period of 2015–2023 for the Can Tho, Hau Giang, and Soc Trang provinces with the research of Kumar et al. (2024).

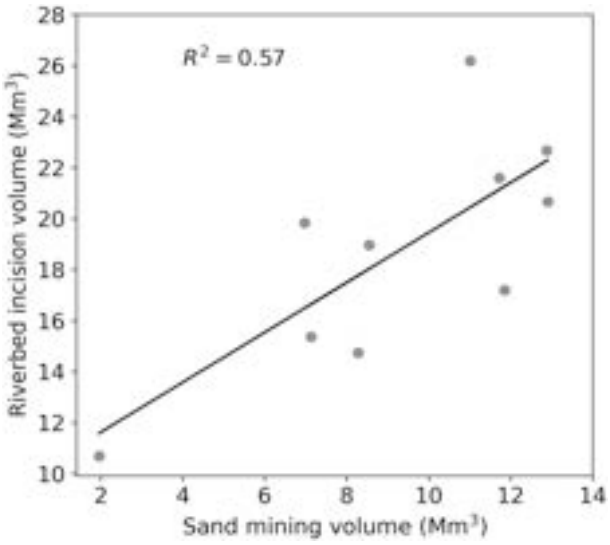

Fig. 17. Correlation between annual sand mining volume and annual riverbed incision volume in 2014–2023 in Sc1.

and maximum volumes of sand mined, thereby reducing potential errors. Fourth, we also assumed an exploitation time of 10 h per day, following government regulation (Nguyen, 2020). However, field observations show that BCs often paused operations when STBs entered and exited to collect sand, meaning the actual exploitation time was lower. In addition, another factor affecting mining duration is the number of active mining days per month. While official licensing documents often assume continuous operation and calculate authorized extraction volumes accordingly (Ngan, 2023; Dang, 2024), actual mining days may be fewer due to equipment failures or adverse weather. As Sentinel imagery does not provide complete daily coverage to accurately determine the number of mining days, we assumed that sand mining activities occurred every day of the month. Therefore, the sand mining volumes estimated in our study represent the maximum extraction capacity of the sites per year. Finally, the dredging and dumping module simulates sand mining activities across the entire sand mine area based on predefined criteria and automatically estimates the daily mining volume for the mining area. Although the model does not allow proactively setting up daily mining volume changes, it effectively reflects the sand mining impacts through daily volume variations and the close agreement between simulated and estimated total mining volumes. Additionally, the dredging module does not fully capture sediment replenishment processes because if natural deposition occurs within the mining area, the deposited sediment is removed again, either partly or entirely, depending on dredge depth and the maximum extraction limit. This differs from natural conditions, where replenishment may remain in place rather than being removed. Nevertheless, these limitations are relatively minor, as the approach still reproduces sand mining activities with reasonable realism. Despite these uncertainties and assumptions, our results are broadly consistent with previous research, supporting the validity of our approach and its relevance for large-scale river sediment management.

This study highlights that sand mining is one of the main drivers causing the current riverbed incision in the VMD. The research, such as Jordan et al. (2019), Hackney et al. (2020), Lau et al. (2023), and Kumar et al. (2024), emphasizes that current sand mining practices in the VMD are unsustainable, with extraction rates exceeding natural replenishment. This underscores the urgent need for policies that balance socio-economic demands with ecological resilience. However, large-scale infrastructure projects, such as the Chau Doc–Can Tho–Soc Trang highway construction, continue to drive significant demand for sand. Therefore, a complete ban on extraction is neither feasible nor realistic; instead, sand mining should be regulated under a sustainable framework. Key measures include evaluating extraction potential and setting science-based quotas, identifying spatial zones where extraction causes less environmental damage, and defining temporal phases of allowable exploitation. These directions also form the outlook for future works. Furthermore, future research should integrate river morphology modeling with socio-economic assessments to inform adaptive management strategies. This would ensure that sand mining, while meeting development needs, is conducted within limits that preserve the long-term stability of riverbeds, banks, and associated ecosystems in the VMD.

6. Conclusion

This research presents a comprehensive methodology to monitor and assess the impacts of sand mining on river morphology in the Bassac River in the Vietnamese Mekong Delta (VMD) by using deep learning, satellite imagery, and numerical simulations (Delft3D).

From 2014 to 2023, 386 barges with crane (BC) boats were detected along the Bassac River. Based on estimated mining capacities and operation durations, the total sand extraction volume was calculated at 92.68–137.59 Mm^3, with an annual average of 10.02–14.87 Mm^3.

Morphodynamic simulations revealed that sand mining profoundly altered riverbed morphology. The maximum annual net incision volume reached −29.48 Mm^3/yr, with a mean incision rate of up to −0.82 m/yr. Moreover, excessive sand mining formed twenty-three scour holes with depths up to 11 m and incised the thalweg at rates of up to −1.18 m/yr, particularly at the sand mining sites, river confluences, and meandering segments. Scour hole formation and thalweg migration toward riverbanks significantly undermined bank stability, threatening communities along the river. Furthermore, the study estimates that sand mining was at most responsible for 41.0–56.4 % of total riverbed incision during 2014–2023.

These results underscore the urgent need for improved sediment management strategies and regulatory frameworks to mitigate the environmental impacts of excessive sand extraction. Future research should prioritize the development of sustainable sand mining policies to ensure the long-term stability of the Bassac River and the resilience of its associated ecosystems.

CRediT authorship contribution statement

Thi Huong Vu: Writing – original draft, Software, Methodology, Investigation, Formal analysis. **Lars Backhaus:** Writing – review & editing, Validation, Software, Methodology, Data curation. **Doan Van Binh:** Writing – review & editing, Resources, Methodology, Data curation. **Sameh Ahmed Kantoush:** Writing – review & editing, Resources, Data curation. **Jürgen Stamm:** Writing – review & editing, Supervision.

Declaration of competing interest

The authors declare the following financial interests/personal relationships which may be considered as potential competing interests: Thi Huong Vu reports that financial support was provided by the Katholischer Akademischer Ausländer-Dienst (KAAD) scholarship program in Germany. Doan Van Binh reports that financial support was provided by the Japan ASEAN Science, Technology and Innovation Platform (JASTIP). Doan Van Binh reports that financial support was provided by the Asia-Pacific Network for Global Change Research (APN). If there are other authors, they declare that they have no known competing financial interests or personal relationships that could have appeared to influence the work reported in this paper.

Acknowledgments

This study is funded by the Katholischer Akademischer Ausländer-Dienst (KAAD) scholarship program in Germany. Doan Van Binh received support from the Asia-Pacific Network for Global Change Research (APN) under project reference number CRRP2023-04MY-Doan Van (Funder ID: doi:1 0.13039/100005536) and the Japan-ASEAN Science, Technology and Innovation Platform (JASTIP) project of Kyoto University. We acknowledge Mr. Huan Ngoc Tran at Institute of ecological research and planning, Germany, for providing valuable comments to improve the paper quality.

Appendix A. Supplementary data

Supplementary data to this article can be found online at https://doi.org/10.1016/j.geomorph.2025.110010.

Data availability

Data will be made available on request.

References

Ahmed, M.F., Van Binh, D., Kantoush, S.A., Park, E., Doan, N.L.P., Tuan, L.A., Dinh, V.N., Vu, T.H., Nguyen, B.Q., Ngoc, T.A., Tung, N.X., Sumi, T., 2025. Intensified susceptibility to riverbed incisions under sand mining impacts in the Vietnamese Mekong Delta: a long-term spatiotemporal analysis. Geomorphology 470. https://doi.org/10.1016/j.geomorph.2024.109535.

Anthony, E.J., Brunier, G., Besset, M., Goichot, M., Dussouillez, P., Nguyen, V.L., 2015. Linking rapid erosion of the Mekong River delta to human activities. Sci. Rep. 5. https://doi.org/10.1038/srep14745.

Binh, D.V., Kantoush, S.A., Ata, R., Tassi, P., Nguyen, T.V., Lepesqueur, J., Abderrezzak, K.E.K., Bourban, S.E., Nguyen, Q.H., Phuong, D.N.L., Trung, L.V., Tran, D.A., Letrung, T., Sumi, T., 2022. Hydrodynamics, sediment transport, and morphodynamics in the Vietnamese Mekong Delta: field study and numerical modelling. Geomorphology 413. https://doi.org/10.1016/j.geomorph.2022.108368.

Binh, D.V., Kantoush, S.A., Saber, M., Mai, N.P., Maskey, S., Phong, D.T., Sumi, T., 2020a. Long-term alterations of flow regimes of the Mekong River and adaptation strategies for the Vietnamese Mekong Delta. J. Hydrol. Reg. Stud. 32, 100742. https://doi.org/10.1016/j.ejrh.2020.100742.

Binh, D.V., Kantoush, S., Sumi, T., 2020b. Changes to long-term discharge and sediment loads in the Vietnamese Mekong Delta caused by upstream dams. Geomorphology 353, 107011. https://doi.org/10.1016/j.geomorph.2019.107011.

Binh, D.V., Kantoush, S.A., Sumi, T., Mai, N.P., Ngoc, T.A., Trung, L.V., An, T.D., 2021. Effects of riverbed incision on the hydrology of the Vietnamese Mekong Delta. Hydrol. Process. 35, 1–21. https://doi.org/10.1002/hyp.14030.

Bravard, J.-P., Goichot, M., Gaillot, S., 2013. Geography of sand and Gravel Mining in the Lower Mekong River. EchoGéo. https://doi.org/10.4000/echogeo.13659.

Consult, Brockmann, 2015. SNAP 8.0 released – STEP [WWW Document]. URL. https://step.esa.int/main/snap-8-0-released/ accessed 5.4.25.

Brunier, G., Anthony, E.J., Goichot, M., Provansal, M., Dussouillez, P., 2014. Recent morphological changes in the Mekong and Bassac river channels, Mekong delta: the marked impact of river-bed mining and implications for delta destabilisation. Geomorphology 224, 177–191. https://doi.org/10.1016/j.geomorph.2014.07.009.

Dang, N.A., Benavidez, R., Tomscha, S.A., Nguyen, H., Tran, D.D., Nguyen, D.T.H., Loc, H.H., Jackson, B.M., 2021. Ecosystem service modelling to support nature-based flood water management in the Vietnamese Mekong River Delta. Sustain 13, 1–28. https://doi.org/10.3390/su132413549.

Dang, T., 2024. Starting to exploit two sand mines to supply Cao Lanh - An Huu expressway [WWW Document]. URL. https://tuoitre.vn/bat-dau-khai-thac-hai-mo-cat-cung-ung-cao-toc-cao-lanh-an-huu-20240516101442497.htm accessed 10.1.24.

Darby, S.E., Hackney, C.R., Leyland, J., Kummu, M., Lauri, H., Parsons, D.R., Best, J.L., Nicholas, A.P., Aalto, R., 2016. Fluvial sediment supply to a mega-delta reduced by shifting tropical-cyclone activity. Nature 539, 276–279. https://doi.org/10.1038/nature19809.

Day, J.W., Agboola, J., Chen, Z., D'Elia, C., Forbes, D.L., Giosan, L., Kemp, P., Kuenzer, C., Lane, R.R., Ramachandran, R., Syvitski, J., Yañez-Arancibia, A., 2016. Approaches to defining deltaic sustainability in the 21st century. Estuar. Coast. Shelf Sci. 183, 275–291. https://doi.org/10.1016/j.ecss.2016.06.018.

Deltares, 2024. 3D/2D Modelling Suite for Integral Water Solutions, DELFT3D-FLOW. Boussinesqweg 1 2629 HV Delft P.O. 177 2600 MH Delft Netherlands 1–110.

ESA, 2014. Sentinel-1 - Sentinel Online [WWW Document]. URL. https://sentinels.copernicus.eu/copernicus/sentinel-1 accessed 5.4.25.

Eslami, S., Hoekstra, P., Nguyen Trung, N., Ahmed Kantoush, S., Van Binh, D., Duc Dung, D., Tran Quang, T., van der Vegt, M., 2019. Tidal amplification and salt intrusion in the Mekong Delta driven by anthropogenic sediment starvation. Sci. Rep. 9, 1–11. https://doi.org/10.1038/s41598-019-55018-9.

Ferrarin, C., Madricardo, F., Rizzetto, F., Mc Kiver, W., Bellafiore, D., Umgiesser, G., Kruss, A., Zaggia, L., Foglini, F., Ceregato, A., Sarretta, A., Trincardi, F., 2018. Geomorphology of scour holes at tidal channel confluences. Case Rep. Med. 123, 1386–1406. https://doi.org/10.1029/2017JF004489.

Ferrer, L.M., Rodriguez, D.A., Forti, M.C., Carriello, F., 2021. The anthropocene landscape and ecosystem services in the closure of sand mining: Paraíba do Sul River basin – Brazil. Res. Policy 74. https://doi.org/10.1016/j.resourpol.2021.102405.

Gruel, C.R., Park, E., Switzer, A.D., Kumar, S., Loc Ho, H., Kantoush, S., Van Binh, D., Feng, L., 2022. New systematically measured sand mining budget for the Mekong Delta reveals rising trends and significant volume underestimations. Int. J. Appl. Earth Obs. Geoinf. 108. https://doi.org/10.1016/j.jag.2022.102736.

Gugliotta, M., Saito, Y., Nguyen, V.L., Ta, T.K.O., Nakashima, R., Tamura, T., Uehara, K., Katsuki, K., Yamamoto, S., 2017. Process regime, salinity, morphological, and sedimentary trends along the fluvial to marine transition zone of the mixed-energy Mekong River delta, Vietnam. Cont. Shelf Res. 147, 7–26. https://doi.org/10.1016/j.csr.2017.03.001.

Hackney, C.R., Darby, S.E., Parsons, D.R., Leyland, J., Best, J.L., Aalto, R., Nicholas, A.P., Houseago, R.C., 2020. River bank instability from unsustainable sand mining in the lower Mekong River. Nat. Sustain. 3, 217–225. https://doi.org/10.1038/s41893-019-0455-3.

Hackney, C.R., Vasilopoulos, G., Heng, S., Darbari, V., Walker, S., Parsons, D.R., 2021. Sand mining far outpaces natural supply in a large alluvial river. Earth Surf. Dyn. 9, 1323–1334. https://doi.org/10.5194/esurf-9-1323-2021.

Hung, N.N., Delgado, J.M., Güntner, A., Merz, B., Bárdossy, A., Apel, H., 2014. Sedimentation in the floodplains of the Mekong Delta, Vietnam Part II: Deposition and erosion. Hydrol. Process. 28, 3145–3160. https://doi.org/10.1002/hyp.9855.

Huy, N.H.T., 2017. Each Sand Dredger earns hundreds of millions of Dong every Day [WWW Document]. URL. https://cand.com.vn/dieu-tra-theo-don-ban-doc/Ky-2-Moi-tau-hut-cat-kiem-ca-tram-trieu-dong-moi-ngay-i431457/.

Jocher, G., Stoken, A., Chaurasia, A., Borovec, J., NanoCode012, TaoXie, Kwon, Y., Michael, K., Changyu, L., Fang, J., V, A., Laughing, tkianai, yxNONG, Skalski, P., Hogan, A., Nadar, J., imyhxy, Mammana, L., AlexWang1900, Fati, C., Montes, D., Hajek, J., Diaconu, L., Minh, M.T., Marc, albinxavi, fatih, oleg, wanghaoyang0106, 2021. ultralytics/yolov5: v6.0 - YOLOv5n "Nano" models, Roboflow integration, TensorFlow export, OpenCV DNN support. doi:https://doi.org/10.5281/ZENODO.5563715.

Jordan, C., Tiede, J., Lojek, O., Visscher, J., Apel, H., Nguyen, H.Q., Quang, C.N.X., Schlurmann, T., 2019. Sand mining in the Mekong Delta revisited - current scales of local sediment deficits. Sci. Rep. 9, 1–14. https://doi.org/10.1038/s41598-019-53804-z.

Jordan, C., Visscher, J., Dung, N.V., Apel, H., Schlurmann, T., 2020. Impacts of human activity and global changes on future morphodynamics within the Tien River, Vietnamese Mekong Delta. Water (Switzerland) 12. https://doi.org/10.3390/w12082204.

Kim, T.T., Nga, T.N.Q., Huy, N.D.Q., Phung, N.K., Hoai, H.C., Bay, N.T., 2025. The impact of sand mining on the bed morphology of the Tien River, Mekong Delta, Vietnam. Environ. Earth Sci. 84. https://doi.org/10.1007/s12665-024-12079-y.

Koehnken, L., 2014. Discharge sediment monitoring project (DSMP) 2009–2013 summary & analysis of results. Mekong River Comm, p. 126.

Kondolf, G.M., 1997. Hungry water: effects of dams and gravel mining on river channels.

Kumar, S., Park, E., Tran, D.D., Wang, J., Loc Ho, H., Feng, L., Kantoush, S.A., Van Binh, D., Li, D., Switzer, A.D., 2024. A deep learning framework to map riverbed sand mining budgets in large tropical deltas. GIScience Remote Sens. 61. https://doi.org/10.1080/15481603.2023.2285178.

Lau, R.Y.S., Park, E., Koh, Y.Q., Tran, D.D., Kantoush, S.A., Van Binh, D., Loc, H.H., 2024. Recurrence interval of riverbed sand mining hotspots in the Mekong delta: potential indications of unsustainable replenishment rates. J. Environ. Manag. https://doi.org/10.1016/j.jenvman.2024.122435.

Lau, R.Y.S., Park, E., Tran, D.D., Wang, J., 2023. Recent intensification of riverbed mining in the Mekong Delta revealed by extensive bathymetric surveying. J. Hydrol. 626, 130174. https://doi.org/10.1016/j.jhydrol.2023.130174.

Loc, H.H., Van Binh, D., Park, E., Shrestha, S., Dung, T.D., Son, V.H., Truc, N.H.T., Mai, N.P., Seijger, C., 2021. Intensifying saline water intrusion and drought in the Mekong Delta: from physical evidence to policy outlooks. Sci. Total Environ. 757, 143919. https://doi.org/10.1016/j.scitotenv.2020.143919.

Ngan, H., 2023. How is the special sand mine for highway construction being exploited [WWW Document]. https://baoxaydung.vn/mo-cat-dac-thu-lam-cao-toc-dang-khai-thac-the-nao-192231024003819755.htm accessed 11.23.24.

Nguyen, B.Q., Kantoush, S.A., Sumi, T., 2025. Assessing the multidimensional impacts of riverbed sand mining on geomorphological change and water transfer rate: a comprehensive investigation of Central Vietnam's Vu Gia Thu Bon River system. J. Hydrol., 132853 https://doi.org/10.1016/j.jhydrol.2025.132853.

Nguyen, X.P., 2020. Decree No. 23/2020/ND-CP Of the Government: Management of riverbed sand and gravel and protection of riverbed, banks and terraces 25, 1–9.

Park, E., 2024. Sand mining in the Mekong Delta: Extent and compounded impacts. Sci. Total Environ. https://doi.org/10.1016/j.scitotenv.2024.171620.

Quan, N.H., Toan, T.Q., Dang, P.D., Phuong, N.L., Anh, T.T.H., Quang, N.X., Quoc, D.P., Quoi, L.P., Hanington, P., Sea, W.B., 2018. Conservation of the Mekong Delta wetlands through hydrological management. Ecol. Res. 33, 87–103. https://doi.org/10.1007/s11284-017-1545-1.

Ren, Y., Li, X., Xu, H., 2022. A Deep Learning Model to Extract Ship size from Sentinel-1 SAR Images. IEEE Trans. Geosci. Remote Sens. 60, 1–14. https://doi.org/10.1109/TGRS.2021.3063216.

Roy, Pulaha, Agarwal, Siddharth, Anirvan, K., 2023. These Satellite Images of Indian Rivers Highlight Environmental Impacts of Sand Mining [WWW Document]. URL. https://www.downtoearth.org.in/mining/these-satellite-images-of-indian-rivers-highlight-environmental-impacts-of-sand-mining-88868.

Stephens, J.D., Allison, M.A., Di Leonardo, D.R., Weathers, H.D., Ogston, A.S., McLachlan, R.L., Xing, F., Meselhe, E.A., 2017. Sand dynamics in the Mekong River channel and export to the coastal ocean. Cont. Shelf Res. 147, 38–50. https://doi.org/10.1016/j.csr.2017.08.004.

Thanh, V.Q., Roelvink, D., van der Wegen, M., Reyns, J., van der Spek, A., Van Vinh, G., Phuong Linh, V.T., Tu, L.X., Trung, N.H., 2025. A numerical investigation on the suspended sediment dynamics and sediment budget in the Mekong Delta. Cont. Shelf Res. 286. https://doi.org/10.1016/j.csr.2025.105427.

Truong, M., 2024. Tien Giang starts operation of first sand mine to supply for Ho Chi Minh City Ring Road 3 project [WWW Document]. URL. https://tuoitre.vn/tien-giang-khoi-cong-mo-cat-dau-tien-cung-cap-cho-du-an-duong-vanh-dai-3-tp-hcm-20241009170419512.htm accessed11.23.24.

Tzutalin, 2015. GitHub - HumanSignal/labelImg [WWW Document]. URL. https://github.com/HumanSignal/labelImg accessed 5.6.25.

Ultralytics, 2022. GitHub - ultralytics/yolov5 [WWW Document]. URL. https://github.com/ultralytics/yolov5 accessed 7.23.24.

UNEP, 2023. Sand mining: how it impacts the environment and solutions | World Economic Forum [WWW Document]. URL. https://www.weforum.org/stories/2023/09/global-sand-mining-demand-impacting-environment/ accessed 5.6.25.

Vu, T.H., Binh, D.V., Tran, H.N., Khan, M.A., Du Bui, D., Stamm, J., 2024. Quantifying spatio-temporal river morphological change and its consequences in the Vietnamese Mekong River Delta using remote sensing and geographical information system techniques. Remote Sens 16, 1–27. https://doi.org/10.3390/rs16040707.

Wang, Z., Men, S., Bai, Y., Yuan, Y., Wang, J., Wang, K., Zhang, L., 2024. Improved small object detection algorithm crl-yolov5. Sensors 24, 1–12. https://doi.org/10.1109/MIS.2024.3399053.

Wen, Z., Lu, J., Wan, Z., Gao, X., Huang, Z., Xiao, Y., Liu, J., 2025. Thalweg migration under the collaborative changes in the hydro-sediment regime and erosion base level in the Xiaobeiganliu reach of the Middle Yellow River. J. Geogr. Sci. 35, 1516–1532. https://doi.org/10.1007/s11442-025-2382-8.

WMF, 2018. As sand mining grows, Asia's deltas are sinking, water experts warn | PreventionWeb [WWW Document]. URL. https://www.preventionweb.net/news/sand-mining-grows-asias-deltas-are-sinking-water-experts-warn.

Xin, S.L.C., Park, E., Tran, D.D., Yuen, K.W., Wang, J., 2024. Landscape and Social Disruption from Sand Mining and Mining-Related Activities: a Case from the Vietnamese Mekong Delta. Ann. Am. Assoc. Geogr. 114, 1968–1984. https://doi.org/10.1080/24694452.2024.2366899.

Yuen, K.W., Park, E., Tran, D.D., Loc, H.H., Feng, L., Wang, J., Gruel, C.R., Switzer, A.D., 2024. Extent of illegal sand mining in the Mekong Delta. Commun. Earth Environ. 5, 1–13. https://doi.org/10.1038/s43247-023-01161-1.

Zhang, M., Feng, X., Yan, T., Wang, X., 2022. Human impacts on riverbed morphology and hydrology in the lower reaches of the West River, China. River Res. Appl. 38, 952–964. https://doi.org/10.1002/rra.3960.